UNIVERSITY OF
CAMBRIDGE
Department of Engineering

Optimal Siting of Energy Storage in Fully Renewable Power Grids

A convex semi-definite program formulation via an exact multi-period optimal power flow relaxation dual

Author name: Max Langtry

Supervisor: Ioannis Lestas

Date: 1st June, 2021

I hereby declare that, except where specifically indicated, the work submitted herein is my own original work.

Signed: 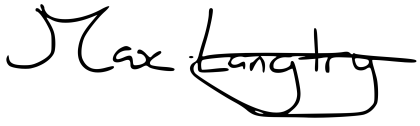

Date: 1st June, 2021

Optimal Siting of Energy Storage in Fully Renewable Power Grids

A convex semi-definite program formulation via an exact multi-period optimal power flow relaxation dual

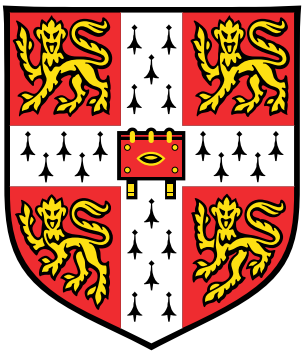

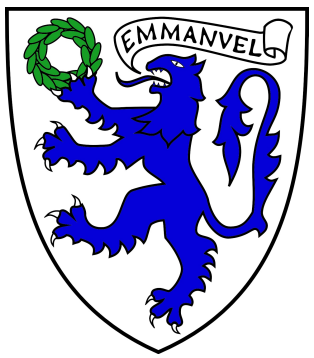

Max Langtry

Department of Engineering
University of Cambridge

This dissertation is submitted for the degree of
Master's of Engineering

Emmanuel College

June 2021

Declaration

I hereby declare that except where specific reference is made to the work of others, the contents of this dissertation are original and have not been submitted in whole or in part for consideration for any other degree or qualification in this, or any other university. This dissertation is my own work and contains nothing which is the outcome of work done in collaboration with others, except as specified in the text and Acknowledgements. This dissertation, excluding front matter, contains not more than 12,000 words[1] including appendices, footnotes, captions, and tables, but excluding references, and is not more than 50 pages long.

Max Langtry
June 2021

[1] As determined by TEXcount

Acknowledgements

I would like to thank Dr Lestas for his encouragement and guidance throughout this project, for which I am extremely grateful, and Jeremy Watson for giving his time so generously and providing a wealth insightful suggestions.

CONTENTS

Technical Abstract

Transitioning to fully renewable electricity generation will play a critical role in achieving substantive reductions in carbon emissions arising from energy usage, and is increasingly important in light of recent trends towards the electrification of the transportation and heating sectors. However, integrating renewable generation into modern power systems presents a number of significant challenges, arising from the uncontrollability, variability, and poor predictability of many prominent renewable sources. These undesirable supply characteristics necessitate the widespread usage of auxiliary power system support infrastructure, such as energy storage & arbitrage, demand-side response, and sector coupling, to support fully renewable generation, so that system stability, security of supply, and a viable system cost of provision can be maintained. Due to the uncontrollable, unpredictable nature of wind and solar generation, the predominant renewable sources in the UK, ensuring instantaneous supply-demand matching at all times in a high penetration renewable power system requires some combination of over-capacity of generation and energy storage.

Optimisation techniques will play a key role in facilitating the transition to renewables, by identifying robust, cost effective system development and operation strategies, thereby reducing the cost of, and risk associated with, the transition. These optimisation methods must be highly computationally efficient in order to facilitate the extended simulation durations required to accurately represent long term system behaviour. Further, they must be able to appropriately model the localisation effects within the power network, so that the potentially critical transmission loss information can be incorporated into the development and operational strategies determined.

However, modern power system optimisation tools [1]–[3] linearise the power network physics, losing localisation effect information in the process, and limiting their ability to identify true optimal strategies. In contrast, optimal power flow literature [4]–[10] proposes a number of formulations which allow for power system operating point optimisation problems with fully complexity network physics to be solved via a convex optimisation. This work seeks to adapt such convex formulations to full complexity power system infrastructure development strategy optimisation problems. This class of problems aims to determine the power system infrastructure asset configuration which minimises the overall cost of satisfying electricity demand, and therefore requires the use of system parameters which define the operational constraints of the network as decision variables. The objectives used embody some aspect of the overall cost of electricity provision, and are optimised over both the system configuration and operation strategy. This is distinct from classical optimal power flow problems, which are concerned only with identifying the optimal operation strategy for a given power system configuration. The development of a convex formulation for this class of problems would provide a solution method which accurately represents localisation effects within power networks, whilst also giving computational efficiency, global optimality, and solution accuracy guarantees.

The formulation is approached via the extension of the convex optimal power flow formulations presented by Lavaei & Low [4] and Gayme & Topcu [5] to system development optimisation. The solution strategy utilises the dual of a convex relaxation of the original problem, which takes the form of a convex semi-definite program, to solve the optimisation problem. The global optimum solution can be retrieved from the solution to the dual problem when the duality gap is zero, i.e. the dual solution is exact, and [4] proves necessary and sufficient conditions for exactness of the dual solution in the single period case.

This work presents a description of the power system optimisation problem, and the mathematics of the full complexity network power flow physics. From this, strategies for problem convexification via the simplification of said physics are discussed, demonstrating

the breadth of potential formulations and their characteristics.

The extension of the SDP relaxation dual formulation to the multi-period problem is derived and shown to proceed in a similar manner to that in [4], and its convexity is verified by noting that it retains the SDP form. Further, the conditions for exactness of the dual solution are proved to extend to the multi-period case. This formulation is found to have a number of interesting structural properties. Critically, the aggregate Lagrange multiplier dual variables corresponding to the voltage matrix primal variables are shown to be separable in time. This provides a basis for the proof of the extended conditions for exactness, and results in the ability to add any further affine system dynamics without altering the nature of the dual problem and the associated exactness conditions, as well as a 'super sparse' structure of the dual problem, demonstrated in Fig. 4.

Primal solution recovery strategies for the case in which the exactness conditions are satisfied, based off that proposed in [5], and the non-exact dual solution case, are presented, with the attempted recovery in the non-exact case taking the form of a SDP relaxation of a rank minimisation problem. However, whilst the exact recovery is found to perform well, the non-exact recovery fails to yield primal approximations which are both feasible and consistent with the objective in practice.

Numerical experiments performed on a simplified model of the UK transmission level power system, shown in Fig. 1, utilising renewable generation power data synthesised from historic meteorological observations [11] and appropriate technology models [12], [13], novelly demonstrate that the conditions for exactness can be satisfied by the UK power network topology. As justified in [4], this provides a pathway for obtaining arbitrarily accurate approximate solutions to the original problem on the network topology for arbitrary power time series in polynomial time, via the convex ε-modified problem, which achieves zero duality gap. Further, these experiments demonstrate the formulation's ability to determine the global optimum solution in polynomial time, finding the computational complexity in the observation duration to be $O(T^3)$.

A number of extensions to the model are proposed, which illustrate how the formulation can be extended to a fully-featured power system optimisation tool, by exploiting the retention of the conditions for exactness with the addition of further affine system dynamics.

This work demonstrates that optimisation formulations and solution techniques from optimal power flow literature can be adapted to solve renewable power system optimisation problems, providing a convex method for solving this class of problems, whilst accounting for the full complexity power network physics. Such convexity is critical, as it guarantees global optimality and provides computationally efficient, provably polynomial time, algorithms for determining said optimal solution. This allows for the development of power system optimisation tools which more accurately model the localisation effects in power transmission, and hence provide system development and operational strategies which account for this potentially critical network effect. These improved strategies help reduce the risk and cost associated with a transition to fully renewable electricity generation, and thus accelerate progress towards net zero carbon emissions.

I. Introduction

In order to achieve substantial reductions in carbon emissions arising from energy usage, a transition to high proportions of renewable energy generation will be necessary. However, integrating renewable generation into modern power systems, and ultimately transitioning to a fully renewable electricity network, whilst maintaining security of supply and viable system operation cost presents significant challenges. These arise from the uncontrollability, variability, and poor predictability of many prominent renewable sources. These challenges are especially prevalent in the UK, which utilises primarily wind and solar generation, both of which suffer from high magnitude, high frequency variability, and poor predictability beyond aggregate capacity factors. Potential auxiliary technologies for supporting renewable generation include energy storage, demand-side response, and sector coupling, which is especially important in light of recent trends towards the electrification of the transportation and heating sectors.

In order to ensure security of supply for the consumer, power systems must be designed so that electricity demand can be satisfied instantaneously at all times. Due to the uncontrollable nature of wind and solar, achieving supply-demand balancing in a fully renewable grid requires some combination of over-capacity of generation and energy storage for temporal arbitrage. Extreme over-capacity results in substantial cost inefficiency due to under-utilisation of energy generation potential, and hence energy arbitrage may provide a more economical operation scheme by shifting renewably generated energy in time to match demand.

Optimisation techniques will play a key role in minimising both the cost and energy security impacts of a transition to renewable energies, through the identification of robust, minimal cost infrastructure development and operational strategies for transitioning power systems. These optimisation methods must be highly computationally efficient in order to allow the solution of problems over the extended simulation durations required to accurately represent long term system behaviour to be tractable. Further, as grid interconnectivity and diversity of renewable supply are likely to provide substantial system stability and cost benefits to future power systems, said optimisation techniques must be able to accurately model the true behaviour of, and losses associated with, power transmission over long distances, to account for the critical network localisation effects in system operation strategies.

However, modern power system optimisation tools [1]–[3] do not account for the full complexity power network physics, instead linearising the power flow equations, losing potentially crucial information on transmission localisation effects in the process. Optimal power flow literature [4]–[10] presents a potential pathway to introducing non-linear line loss information to power systems optimisation problems whilst maintaining the required computational efficiency, as it provides formulations which convexify power system operating point optimisation problems, subject to the full complexity network physics. Power systems optimisation problems aim to determine the power system infrastructure asset configuration which minimises the overall cost of satisfying electricity demand, and therefore require the use of system parameters which define the operational constraints of the network as decision variables. The objectives used embody some aspect of the overall cost of electricity provision, and are optimised over both the system configuration and operation strategy. This is distinct from classical optimal power flow problems, which are concerned only with identifying the optimal operation strategy for a given power system configuration. Adaptation of these convex formulations to full complexity power system optimisation problems would yield solution methods for this class of problems which accurately represent localisation effects within power networks, whilst also giving computational efficiency, global optimality, and solution accuracy guarantees.

This work seeks to extend the optimal power flow formulations presented by Lavaei & Low [4] and Gayme & Topcu [5] to the context of renewable power system development and operational strategy optimisation. These papers propose a solution strategy by which the optimal solution to the optimal power flow problem is determined from the dual of a rank relaxation of the original problem, with both the relaxation and dual taking the form of convex, semi-definite programs. The optimal solution can be recovered whenever the duality gap is zero, and necessary and sufficient conditions for such exactness are proved. Further, these conditions are found to hold widely in practice. This therefore provides a technique for solving the original, non-convex problem via an equivalent convex problem, with polynomial time solution algorithms.

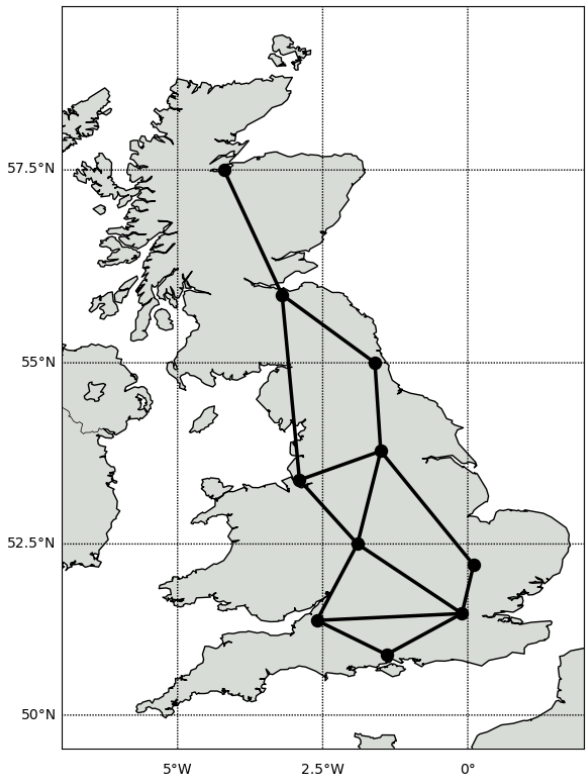

Fig. 1: 10 node representation of UK transmission level power system
Interactive version showing location of data sources available here

This report is structured as follows. Section II defines the renewable power system optimisation and optimal power flow problems, and discusses the variety of solution techniques proposed in the literature. Section III presents the mathematical description of the power network physics used in the formulation, and then demonstrates how its manipulation can yield a number of potential problem convexifications, discussing in each case the merits and flaws. In Section IV, the SDP relaxation dual formulation is derived, necessary and sufficient conditions for zero duality gap proved, and the complete solution recovery strategy presented. Following this, the properties of the dual problem are analysed. Numerical experiments are performed using a Python-based implementation of the optimisation formulation, and their results presented in Section V. These experiments apply the optimisation method to a simplified model of the UK transmission level power system, shown in Fig. 1, over a test time window, using historic renewable power generation and power demand data. As renewable energy generation is currently relatively limited in the UK, the power generation profiles

are synthesised from historic meteorological observation data, taken from the MetOffice's MIDAS dataset [11], and appropriate technology models, in order to provide a reasonable representation of diverse future generation assets. The experimentation investigates the satisfaction of the exactness conditions, and the computational complexity of the proposed solution method. Finally, Section VI demonstrates how the simplified formulation presented in the report can be extended to a fully-featured power system optimisation tool, before concluding remarks are drawn in Section VII.

II. Problem Definition

A. Renewable Power Systems Infrastructure & Operation Optimisation

The fundamental goal of the optimisation method is to use historic power data to identify joint operational and system development strategies which provide an optimal trade-off between incurring line losses in transmission, energy wastage due to over-generation, and under-utilisation of energy storage assets, in order to yield a power system which provides the minimal overall system cost of satisfying electricity demand with solely renewable sources.

Initially, the problem of storage capacity minimisation will be considered in isolation, before then extending the optimisation to include both generation asset implementation strategies, and transmission network development strategies.

Solving this optimisation problem requires the determination of co-optimal system configuration and system operation strategies. The system configuration defines the limits of behaviour of the power transmission network, and hence the system constraints, whilst the system operation strategy involves the distribution of power through the network, subject to the constraints of the system.

Therefore, this problem can be seen to contain a sub-problem of determining the set of network power flows which optimise the objective, subject to the operating constraints of the power system. Thus, it is an instance of a class of optimisation problems known as Optimal Power Flow (OPF) problems.

B. Optimal Power Flow Problems

Optimal power flow problems seek to determine an operating point for a power system which optimises some operational objective, subject to certain constraints on the network power flows. The critical set of constraints are those which represent the (potentially simplified) power transmission physics of the network, with the additional constraint sets chosen as appropriate for the specific problem under consideration. The full complexity network physics constraints are non-linear, and result in a highly non-convex problem.

OPF problems have attracted extensive research interest since Carpentier's seminal work in 1962 [14], with a broad range of formulations and optimisation techniques proposed in the literature, seeking to provide accurate and computationally efficient methods for solving this class of problems. The reviews [15]–[19] provide an overview of the optimisation techniques used in the literature, which include linear programming, Netwon-Raphson, quadratic programming, interior point methods, Lagrange relaxation, particle swarm optimisation, and artificial neural networks, amongst others. Many of these methods are based on the Karush-Kuhn-Tucker (KKT) necessary conditions for constrained optimality, however due to the non-convexity of the full complexity OPF problem, only local optimality can be guaranteed by such methods in these cases.

Substantial research effort has recently been directed at developing computationally efficient solution algorithms with performance guarantees, specifically, a convex formulation of the

OPF problem has been sought. Reference [20] developed a convex OPF problem for radial power networks in the form of a conic program, however this result was shown not to hold for general mesh networks [21]. A convex relaxation in the form of a semi-definite program (SDP) was originally proposed in [22]. Further developments and extensive analyses were made by Lavaei & Low through [4], [6], [7], resulting in a proof of necessary and sufficient conditions to guarantee zero duality gap of the SDP relaxation dual solution, and thus exactness of the SDP relaxation. Further, these conditions were shown to hold widely in practice, and justification provided [4]. This work therefore provides an equivalent convex form of the OPF problem, from which the globally optimal operating point can be determined in a computationally efficient manner, provided the conditions for exactness are satisfied.

Reviews [23] & [24] provide a summary of recent work on convex relaxations of the OPF problem.

C. Multi-Period Optimal Power Flow with Storage Dynamics

Classical OPF problems consider single period, static instances of power flows through a network, and optimise over a single set of power and voltage decision variables, assuming steady-state operation. However, in order to consider the effects of energy storage, the optimisation must be extended to consider the system operation over multiple time instances, to allow the arbitrage of energy over time by the storage units.

To do so, a sequence of single period OPF problems are coupled in time via the states of charge of the storage units in the network by the addition of storage dynamics constraints. The structure of the resulting mutli-period problem is represented in Fig. 2. Note that only the state of charge variables couple the OPF problems between adjacent time instances, and it is this inter-dependence in time that introduces the key aspect of complexity to the multi-period problem.

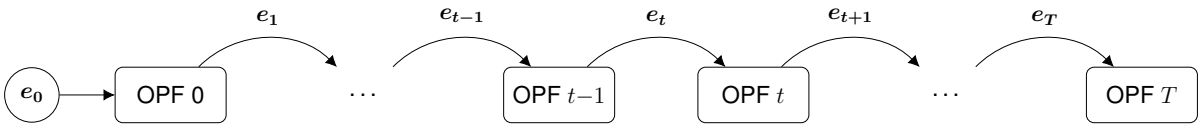

Fig. 2: Structure of multi-period OPF problem with storage dynamics

A number of approaches have been taken to solve multi-period optimal power flow (MOPF) problems in the literature, including linearisation of power flow physics [25], interior point methods [10], and SDP relaxations [26]. Notably, Gayme & Topcu [5] extend the work of Lavaei & Low [4], [6], [7] to multiple period problems, demonstrating the extension of the conditions for exactness of the SDP relaxation dual problem.

D. Contribution to Literature

OPF problems considered in the literature seek to optimise the performance of a given power system subject to some operational conditions [4], [5], and hence are concerned only with operational strategy optimisation.

On the other hand, state-of-the-art power system optimisation tools [1]–[3], which do consider system development strategies, use linearised power flow equations to formulate the problem as a linear program, and exploit the efficiency of linear solvers. However, in

doing so, potentially critical information about the behaviour of power transmission systems is lost[2], and thus the solutions identified may be sub-optimal.

This work seeks to bridge the gap between these two classes of optimisation problem, by developing a convex, full complexity, multi-period OPF problem with a combined operational & development strategy objective. Such a formulation will provide complete, non-linear network physics information, whilst retaining the computational efficiency necessary for solving optimisations over long observation horizons, required to provide valid representations of long-term system operation behaviour, and further provide guarantees on solution accuracy and global optimality.

III. Potential Problem Formulations

As the available historic power system observation data is a set of time series of node generation and demand powers, which yield net bus power injections, the Bus Injection Model (BIM) [23] of network power flow is the natural model for the problem formulation.

The BIM describes the full complexity network power physics, and thus defines the physics constraint set for the optimisation. Additional operational constraints on the power system, such as line capacity constraints and voltage deviation constraints, are included as appropriate to the modelling.

A. The Bus Injection Model

Let the power system be modelled by a connected undirected graph $\mathcal{G}(\mathcal{N}, \mathcal{L})$, where $\mathcal{N} = \{n\}_{n=1}^{N}$ is the set of nodes, each representing a bus in the network, $\mathcal{C}_n \subseteq \mathcal{N} \backslash n = \{k : n \to k\}$ is the set of nodes connected to node n, and $\mathcal{L} = \{(l, m) : l \in \mathcal{N}, m \in \mathcal{C}_l\}$ is the set of transmission lines. For each line $(i, j) \in \mathcal{L}$, let $y_{ij} \in \mathbb{C}$ be its admittance, and I_{ij} the current flowing through it from node i to node j. The complex voltage at bus $k \in \mathcal{N}$ is V_k. Bus 1 is chosen to be the reference bus, and has fixed voltage $V_1 = V_{\text{nom}} \angle 0°$, where V_{nom} is the nominal bus voltage magnitude. Let $s_k = (P_{G,k} - P_{D,k}) + \mathbf{j}(Q_{G,k} - Q_{D,k})$ be the net complex power injection (generation minus load) at bus $k \in \mathcal{N}$.

The BIM is derived by considering power conservation at each node,

$$\underbrace{s_n}_{\text{net power injection}} = \underbrace{\sum_{j \in \mathcal{C}_n} V_n I_{nj}^H}_{\text{power outflow}} \qquad \forall\, n \in \mathcal{N} \tag{1}$$

and applying Ohm's law for line currents,

$$I_{nj} = y_{nj}(V_n - V_j) \tag{2}$$

yielding,

$$s_n = \sum_{j \in \mathcal{C}_n} y_{nj}^H V_n \left(V_n^H - V_j^H \right) \qquad \forall\, n \in \mathcal{N} \tag{3}$$

[2] See online appendix for motivating example calculation.

B. Extension to Multi-Period Bus Injection Model with Storage Dynamics

Multi-period problems consider the operation of a power system over a sequence of time instances $\mathcal{T} = \{t\}_{t=1}^{T}$, with sampling period Δt. At each time instance, t, the instantaneous voltage and bus injection sets must define a valid set of line power flows, i.e. satisfy the physics constraints of the system, (3),

$$s_n{}'[t] = \sum_{j \in \mathcal{C}_n} y_{nj}^H V_n[t] \left(V_n[t]^H - V_j[t]^H \right) \qquad \forall\, n \in \mathcal{N},\, t \in \mathcal{T} \tag{4}$$

However, introduction of energy storage to the system alters the form of the net bus injections, $s_n{}'[t]$. The energy capacity of storage at node n is $S_n \geq 0$, which has state of charge $e_n[t]$ at time t, and initial charge $e_n[0]$, introducing the dummy time period $t = 0$ for notational simplicity. The power flow *into* storage at node n, at time t, is taken as,

$$P_{E,n}[t] = \frac{e_n[t] - e_n[t-1]}{\Delta t} \tag{5}$$

Note that for simplicity the round-trip efficiency of storage is initially neglected. See Section VI-B for the relaxation of this assumption.

Reactive power support $Q_{S,n}[t]$ is assumed available for grid balancing. This results in,

$$\begin{aligned} s_n{}'[t] &= \left(P_{G,n}[t] - P_{D,n}[t] - P_{E,n}[t] \right) + \mathbf{j} \left(Q_{G,n}[t] - Q_{D,n}[t] + Q_{S,n}[t] \right) \\ &= \left(P_{G,n}[t] - P_{D,n}[t] - \frac{e_n[t] - e_n[t-1]}{\Delta t} \right) + \mathbf{j} \left(Q_{G,n}[t] - Q_{D,n}[t] + Q_{S,n}[t] \right) \\ &= s_n[t] - \frac{e_n[t] - e_n[t-1]}{\Delta t} + \mathbf{j} Q_{S,n}[t] \end{aligned} \tag{6}$$

Finally, over the observed duration, the energy levels of storage, $e_n[t]$, must form a consistent set and remain valid, i.e. $0 \leq e_n[t] \leq S_n$.

Therefore, for the multi-period case, the full complexity physics constraints of the system are given by,

$$\begin{aligned} s_n[t] - \frac{e_n[t] - e_n[t-1]}{\Delta t} + \mathbf{j} Q_{S,n}[t] &= \sum_{j \in \mathcal{C}_n} y_{nj}^H V_n[t] \left(V_n[t]^H - V_j[t]^H \right) \\ 0 \leq e_n[t] &\leq S_n \\ &\forall\, n \in \mathcal{N},\, t \in \mathcal{T} \end{aligned} \tag{7}$$

C. Power Balance Slackness

A key feature which differentiates fully renewable power system analysis from classical analysis is the requirement for over-capacity of generation within the system to manage the uncertainty in annual capacity factors, and provide security of supply. As a result, excess energy is generated, and thus at some time instances generation must be curtailed and the ability to generate power foregone. This generation curtailment or 'energy dumping' results in the slack power conservation constraint set,

$$s_n{}'[t] \geq \sum_{j \in \mathcal{C}_n} y_{nj}^H V_n[t] \left(V_n[t]^H - V_j[t]^H \right) \qquad \forall\, n \in \mathcal{N},\, t \in \mathcal{T} \tag{8}$$

These slack power conservation constraints can be shown to be equivalent to the introduction of bounded generation power decision variables, $P_{G,n}^{\min}[t] \leq P_{G,n}[t] \leq P_{G,n}^{\max}[t]$. The time varying upper bound corresponds to the power generation potential profile at bus n, i.e. the maximum available generation power. The lower bound is either $P_{G,n}^{\min}[t] = -P_d$ for the case where active power dumping is available, or $P_{G,n}^{\min}[t] = 0$ otherwise. The single-sided inequality used in (8) corresponds to $P_{G,n}^{\min}[t] = -\infty$, which is reasonable due to the ability to implement sufficient active power dumping via resistance heating of a wastewater pond, turn-up demand-side response (DSR), or sector coupling e.g. district heating.

Power slackness is critical, as it converts the non-convex quadratic power conservation equality constraints to convexifiable quadratic inequality constraints via the implicit introduction of curtailment decision variables.

D. Linearised Power Flow

State-of-the-art power system optimisation tools [1]–[3] convexify the physics constraints by neglecting line losses, hence eliminating the only non-linear aspect of the system constraints, thus converting the problem to a linear program. The linearised slack power conservation constraints are,

$$s_n{}'[t] \geq \sum_{j \in \mathcal{C}_n} s_{nj}[t] \qquad \forall\, n \in \mathcal{N},\, t \in \mathcal{T} \tag{9}$$

where $s_{nj}[t]$ is the complex power flowing through line $n \to j$ at time t. Note, some tools introduce constant line efficiencies [1] to re-introduce some loss information to the problem.

This formulation exploits the computational efficiency of linear programming solvers, making it well suited for solving large-scale problems. However, for national scale power systems, line losses may be a critical localisation effect in power transmission, and hence the removal of this information may result in poor model fit and thus poor solution accuracy.

E. Heuristic Power Flow Convexification

The physics constraints can be convexified whilst retaining the quadratic nature of line losses through formulation as a convex Quadratically Constrained Quadratic Program (QCQP). To do so, a heuristic power flow equation is produced via the assumption that bus voltage deviations from nominal, defined by the reference bus, are negligible. Thus all node bus voltages are taken to be $V_{\text{bus}}\angle 0°$. Hence in this model, approximate line loss information is used, but network voltage information is lost. The resulting slack power conservation constraints are,

$$s_n{}'[t] \geq \sum_{j \in \mathcal{C}_n} \left(V_{\text{bus}}(I_{nj}[t] - I_{jn}[t]) + \left|I_{nj}[t]\right|^2 y_{nj}^{-1} \right) \qquad \forall\, n \in \mathcal{N},\, t \in \mathcal{T} \tag{10}$$

where I_{nj} is now the positive part of the current flowing from $n \to j$, and so $I_{nj} \neq -I_{jn}$.

This can be seen to be a QCQP by comparison to standard form, and convexity follows from the non-negativity of admittance, leading to p.s.d. constraint matrices [27], [28],

$$\sum_{j \in \mathcal{C}_n} \left|I_{nj}\right|^2 y_{nj}^{-1} \to I^H Z_n I \geq 0 \implies Z_n \geq 0$$

This formulation trades off reduced computational efficiency c.f. linearisation with a more accurate representation of network localisation effects.

The form of heuristic used is motivated by the recovery of a global power conservation constraint when summed over all nodes,

$$\underbrace{\sum_{n\in\mathcal{N}} {s_n}'[t]}_{\text{net power in}} \geq V_{\text{bus}} \cancelto{0}{\sum_{n\in\mathcal{N}}\sum_{j\in\mathcal{C}_n}\left(I_{nj}[t] - I_{jn}[t]\right)} + \underbrace{\sum_{n\in\mathcal{N}}\sum_{j\in\mathcal{C}_n}\left|I_{nj}[t]\right|^2 y_{nj}^{-1}}_{\text{total network loss}} \qquad \forall t \in \mathcal{T} \tag{11}$$

F. Exact SDP Rank Relaxation Dual of Bus Injection Model

References [4] & [5] show that a BIM based, full complexity, classical MOPF problem can be brought into matrix form and expressed as a semi-definite program (SDP) subject to rank one constraints on the voltage matrix decision variables. A convex relaxation is produced by eliminating these rank constraints, and the dual of the SDP relaxation, itself a SDP, can be solved. Necessary and sufficient conditions for the dual solution to obtain zero duality gap are proved, and from this exact dual solution the primal solution can be recovered[3]. Further, these conditions for exactness are shown to hold widely in practice for real power systems. Therefore, this formulation provides a convex method for solving full complexity, classical MOPF problems, provided the exactness conditions are satisfied.

This work develops a formulation of this type for the renewable power system optimisation problem defined in Section II. This formulation is specified fully in the following Section.

IV. Optimisation Formulation and Theoretical Results

A. Formulation Structure

The formulation of the SDP relaxation dual problem and proof of necessary and sufficient conditions for exactness is structured following that from [4], shown in Fig. 3, defining Optimisations A through E.

Optimisation A provides the BIM based MOPF problem formulation of the optimisation problem outlined in Section II. This optimisation is then brought into vectorised form, formulating it in terms of the node voltage vectors, producing Optimisation B. The vector terms are then replaced by matrix voltage variables, subject to rank one and positive semi-definiteness constraints, yielding Optimisation C. The rank one constraints are removed to produce the convex relaxation problem, Optimisation D. The dual of Optimisation D, Optimisation E, is then formulated.

The proof of the conditions for exactness proceeds in two stages. Firstly, it is shown that Optimisations D & E satisfy Slater's condition [27], and hence that the duality gap is zero, i.e. Optimisation E is exact w.r.t. Optimisation D. Secondly, it is shown that the proof of the conditions for exactness on the aggregate Lagrange multiplier dual variables corresponding to the voltage matrix primal variables extends to the multi-period case, thus proving necessary and sufficient conditions on the dual solution for the primal, Optimisation D, to have a set of rank one solution matrices, and hence that the relaxation is exact and strong duality holds between Optimisations A & E.

[3] Whilst conditions for exactness on the primal SDP relaxation are proved, simply the primal solution being rank one, solutions satisfying these conditions cannot be practically determined [4], and hence the dual problem is used.

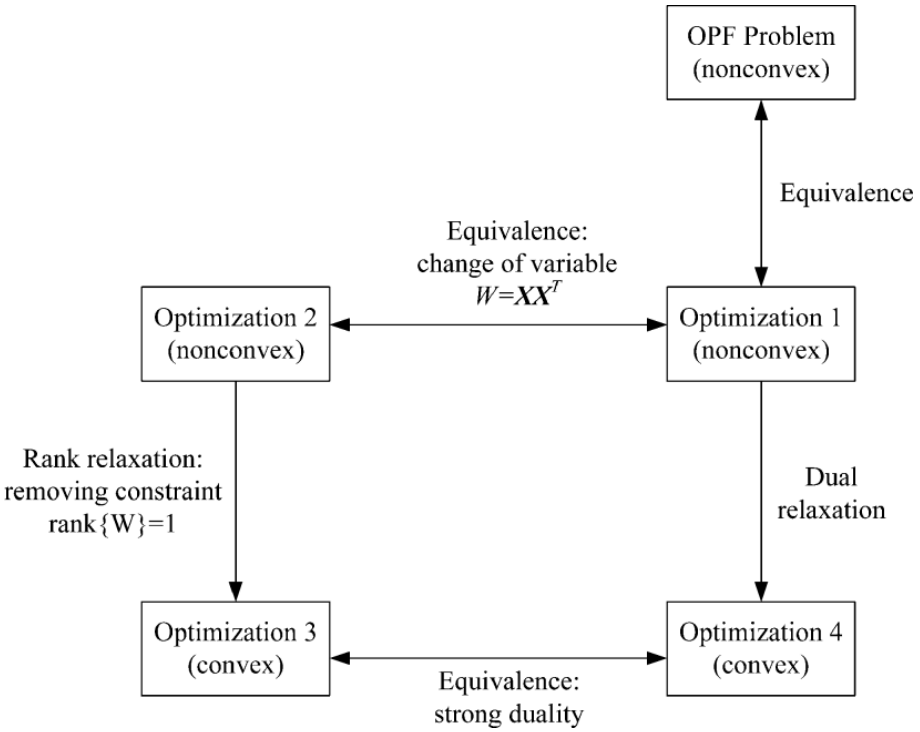

Fig. 3: Structure of single period OPF relaxation dual optimisation formulation and proof of conditions for exactness, Fig. 1 from [4]

B. Mathematical Formulation

The base MOPF problem is defined using the BIM, with the additional application of line power flow constraints and node voltage deviation constraints, as these are important, potentially limiting, localisation effects for the operation of power systems. It is further assumed that active real power dumping is available, and sufficient reactive power support capacity exists as to be non-limiting (effectively unconstrained).

Initially, for simplicity, the simple aggregate installed storage capacity objective function is used. The initial states of charge of the storage units are described by the 'fullness' parameters α_n, $e_n[0] = \alpha_n S_n$. This parametrisation is necessary as the storage capacities S_n are primal decision variables, and thus their values are unknown a priori. Hence the provision of absolute values for the initial states of charge is inappropriate as they cannot be guaranteed to be consistent with the optimised storage capacities, S_n^*, outside the trivial and impractical case $e_n[0] = 0$. Further, for notational simplicity, the sampling frequency of the observed historic power data is defined, $f_s = 1/\Delta t$.

Applying the power slack BIM formulation from Section III-C under the above conditions yields Optimisation A.

Optimisation A:

$$\min \quad \sum_n S_n \tag{12}$$

$$\text{over} \quad S_n, e_n[t], Q_{S,n}[t], V_n[t] \qquad \forall\, n, t$$

$$\text{subject to} \quad \mathrm{Re}\left\{ \sum_{j \in \mathcal{C}_n} y_{nj}^H V_n[t] \left(V_n[t]^H - V_j[t]^H \right) \right\} \leq P_{G,n}[t] - P_{D,n}[t] - f_s(e_n[t] - e_n[t-1]) \tag{12a}$$

$$\mathrm{Im}\left\{ \sum_{j \in \mathcal{C}_n} y_{nj}^H V_n[t] \left(V_n[t]^H - V_j[t]^H \right) \right\} \leq Q_{G,n}[t] - Q_{D,n}[t] + Q_{S,n}[t] \tag{12b}$$

$$\left| y_{lm}^H V_l[t] \left(V_l[t]^H - V_m[t]^H \right) \right| \leq S_{lm}^{\max} \tag{12c}$$

$$V_n^{\min} \leq \left| V_n[t] \right| \leq V_n^{\max} \tag{12d}$$

$$0 \leq e_n[t] \leq S_n \tag{12e}$$

$$S_n \geq 0 \tag{12f}$$

$$\forall\, n \in \mathcal{N},\ (l,m) \in \mathcal{L},\ t \in \mathcal{T}$$

The slack power conservation constraints have been separated into their real and imaginary parts, (12a) and (12b) respectively. The line power flow limits are imposed by constraints on the line apparent power flow magnitude, (12c). (12d) constrains the node voltage magnitude deviations, and (12e) and (12f) impose consistency of energy storage operation, via energy level validity and non-negativity of capacity respectively.

The conversion of Optimisation A into an equivalent rank constrained SDP, Optimisation B, requires the definition of the following network parameters.

Let $\boldsymbol{V}[t] = \left[V_1[t], \ldots, V_N[t] \right]^T$ be the vector of complex node voltages. Let $Y \in \mathbb{C}^{N \times N}$ represent the admittance matrix [4] of the transmission network circuit model, whose (i,j) entry is given by,

$$(Y)_{i,j} = \begin{cases} -y_{ij} & \text{if } i \neq j \\ \sum_{k \in \mathcal{C}_l} y_{ik} & \text{otherwise} \end{cases} \tag{13}$$

where y_{ij} is the admittance of line (i,j) as defined in Section III-A. Further, let $\bar{y}_{ij}$ be its complex conjugate.

Denote the standard basis vectors in $\mathbb{R}^N$ as $e_1, \ldots, e_N$, and define the following matrices for all $k \in \mathcal{N}$, $(i,j) \in \mathcal{L}$, and $t \in \mathcal{T}$:

$$Y_k = e_k e_k^T Y \tag{14a}$$

$$Y_{ij} = (\bar{y}_{ij} + y_{ij}) e_i e_i^T - (y_{ij}) e_i e_j^T \tag{14b}$$

$$\boldsymbol{Y}_k = \frac{1}{2}\begin{bmatrix} \mathrm{Re}\{Y_k + Y_k^T\} & \mathrm{Im}\{Y_k^T - Y_k\} \\ \mathrm{Im}\{Y_k - Y_k^T\} & \mathrm{Re}\{Y_k + Y_k^T\} \end{bmatrix} \tag{14c}$$

$$\boldsymbol{Y}_{ij} = \frac{1}{2}\begin{bmatrix} \mathrm{Re}\{Y_{ij} + Y_{ij}^T\} & \mathrm{Im}\{Y_{ij}^T - Y_{ij}\} \\ \mathrm{Im}\{Y_{ij} - Y_{ij}^T\} & \mathrm{Re}\{Y_{ij} + Y_{ij}^T\} \end{bmatrix} \tag{14d}$$

$$\bar{\boldsymbol{Y}}_k = \frac{-1}{2}\begin{bmatrix} \mathrm{Im}\{Y_k + Y_k^T\} & \mathrm{Re}\{Y_k - Y_k^T\} \\ \mathrm{Re}\{Y_k^T - Y_k\} & \mathrm{Im}\{Y_k + Y_k^T\} \end{bmatrix} \tag{14e}$$

$$\bar{\boldsymbol{Y}}_{ij} = \frac{-1}{2}\begin{bmatrix} \mathrm{Im}\{Y_{ij} + Y_{ij}^T\} & \mathrm{Re}\{Y_{ij} - Y_{ij}^T\} \\ \mathrm{Re}\{Y_{ij}^T - Y_{ij}\} & \mathrm{Im}\{Y_{ij} + Y_{ij}^T\} \end{bmatrix} \tag{14f}$$

$$M_k = \begin{bmatrix} e_k e_k^T & 0 \\ 0 & e_k e_k^T \end{bmatrix} \tag{14g}$$

$$M_{ij} = \begin{bmatrix} (e_i - e_j)(e_i - e_j)^T & 0 \\ 0 & (e_i - e_j)(e_i - e_j)^T \end{bmatrix} \tag{14h}$$

$$\boldsymbol{X}[t] = \begin{bmatrix} \mathrm{Re}\{\boldsymbol{V}[t]\}^T & \mathrm{Im}\{\boldsymbol{V}[t]\}^T \end{bmatrix}^T \tag{14i}$$

Extending *Lemma 1* of [4], the following relationships hold for all $k \in \mathcal{N}$, $(i,j) \in \mathcal{L}$, and $t \in \mathcal{T}$:

$$P_{k,\text{inj}}[t] = \mathrm{Tr}\{\boldsymbol{Y}_k \boldsymbol{X}[t] \boldsymbol{X}[t]^T\} \tag{15a}$$

$$Q_{k,\text{inj}}[t] = \mathrm{Tr}\{\bar{\boldsymbol{Y}}_k \boldsymbol{X}[t] \boldsymbol{X}[t]^T\} \tag{15b}$$

$$P_{ij}[t] = \mathrm{Tr}\{\boldsymbol{Y}_{ij} \boldsymbol{X}[t] \boldsymbol{X}[t]^T\} \tag{15c}$$

$$\left|S_{ij}[t]\right|^2 = \left(\mathrm{Tr}\{\boldsymbol{Y}_{ij} \boldsymbol{X}[t] \boldsymbol{X}[t]^T\}\right)^2 + \left(\mathrm{Tr}\{\bar{\boldsymbol{Y}}_{ij} \boldsymbol{X}[t] \boldsymbol{X}[t]^T\}\right)^2 \tag{15d}$$

$$\left|V_k[t]\right|^2 = \mathrm{Tr}\{M_k \boldsymbol{X}[t] \boldsymbol{X}[t]^T\} \tag{15e}$$

$$\left|V_i[t] - V_j[t]\right|^2 = \mathrm{Tr}\{M_{ij} \boldsymbol{X}[t] \boldsymbol{X}[t]^T\} \tag{15f}$$

$P_{k,\text{inj}}[t]$ and $Q_{k,\text{inj}}[t]$ are the real and reactive net injection powers from external sources to bus k at time t respectively, and are equal to the powers flowing from bus k to the rest of the network through the lines connected to bus k,

$$P_{k,\text{inj}}[t] = P_{k,\text{out}}[t] = P_{G,n}[t] - P_{D,n}[t] - \left(\frac{e_n[t] - e_n[t-1]}{\Delta t}\right) \tag{16a}$$

$$Q_{k,\text{inj}}[t] = Q_{k,\text{out}}[t] = Q_{G,n}[t] - Q_{D,n}[t] + Q_{S,n}[t] \tag{16b}$$

Applying these expressions to the slack power conservation constraints yields,

$$\mathrm{Tr}\{\boldsymbol{Y}_k \boldsymbol{X}[t]\boldsymbol{X}[t]^T\} \leq \underbrace{P_{G,n}[t] - P_{D,n}[t]}_{\text{data}} - \underbrace{\left(\frac{e_n[t] - e_n[t-1]}{\Delta t}\right)}_{\text{storage intake}} \tag{17a}$$

$$\mathrm{Tr}\{\bar{\boldsymbol{Y}}_k \boldsymbol{X}[t]\boldsymbol{X}[t]^T\} \leq \underbrace{Q_{G,n}[t] - Q_{D,n}[t]}_{\text{data}} + \underbrace{Q_{S,n}[t]}_{\text{Q support}} \tag{17b}$$

Using the results from (15d), (15e), (17a), (17b), allows Optimisation A to be re-expressed in vectorised form, as the equivalent Optimisation B.

Optimisation B:

$$\min \quad \sum_n S_n \tag{18}$$

$$\text{over} \quad S_n, e_n[t], Q_{S,n}[t], \boldsymbol{X}[t] \qquad \forall\, n, t$$

$$\text{subject to} \quad \mathrm{Tr}\{\boldsymbol{Y}_n \boldsymbol{X}[t]\boldsymbol{X}[t]^T\} \leq P_{G,n}[t] - P_{D,n}[t] - f_s(e_n[t] - e_n[t-1]) \tag{18a}$$

$$\mathrm{Tr}\{\bar{\boldsymbol{Y}}_n \boldsymbol{X}[t]\boldsymbol{X}[t]^T\} \leq Q_{G,n}[t] - Q_{D,n}[t] + Q_{S,n}[t] \tag{18b}$$

$$\left(\mathrm{Tr}\{\boldsymbol{Y}_{lm} \boldsymbol{X}[t]\boldsymbol{X}[t]^T\}\right)^2 + \left(\mathrm{Tr}\{\bar{\boldsymbol{Y}}_{lm} \boldsymbol{X}[t]\boldsymbol{X}[t]^T\}\right)^2 \leq (S_{lm}^{\max})^2 \tag{18c}$$

$$(V_n^{\min})^2 \leq \mathrm{Tr}\{M_n \boldsymbol{X}[t]\boldsymbol{X}[t]^T\} \leq (V_n^{\max})^2 \tag{18d}$$

$$0 \leq e_n[t] \leq S_n \tag{18e}$$

$$S_n \geq 0 \tag{18f}$$

$$\forall\, n \in \mathcal{N},\ (l,m) \in \mathcal{L},\ t \in \mathcal{T}$$

Optimisation C is produced by performing a change of variables, converting the outer-product terms in the voltage vector variables, $\boldsymbol{X}[t]\boldsymbol{X}[t]^T$, to symmetric voltage matrix variables $W[t]$ subject to rank one and positive semi-definiteness constraints, $\mathrm{rank}\left(W[t]\right) = 1,\ W[t] \succeq 0$.

Optimisation C:

$$\min \quad \sum_n S_n \tag{19}$$

$$\text{over} \quad S_n, e_n[t], Q_{S,n}[t], W[t] \qquad \forall\, n, t$$

$$\text{subject to} \quad \mathrm{Tr}\{\boldsymbol{Y}_n W[t]\} \leq P_{G,n}[t] - P_{D,n}[t] - f_s(e_n[t] - e_n[t-1]) \tag{19a}$$

$$\mathrm{Tr}\{\bar{\boldsymbol{Y}}_n W[t]\} \leq Q_{G,n}[t] - Q_{D,n}[t] + Q_{S,n}[t] \tag{19b}$$

$$\big(\mathrm{Tr}\{\boldsymbol{Y}_{lm} W[t]\}\big)^2 + \big(\mathrm{Tr}\{\bar{\boldsymbol{Y}}_{lm} W[t]\}\big)^2 \leq (S_{lm}^{\max})^2 \tag{19c}$$

$$(V_n^{\min})^2 \leq \mathrm{Tr}\{M_n W[t]\} \leq (V_n^{\max})^2 \tag{19d}$$

$$0 \leq e_n[t] \leq S_n \tag{19e}$$

$$S_n \geq 0 \tag{19f}$$

$$W[t] \succeq 0 \tag{19g}$$

$$\mathrm{rank}\,\big(W[t]\big) = 1 \tag{19h}$$

$$\forall\, n \in \mathcal{N},\ (l,m) \in \mathcal{L},\ t \in \mathcal{T}$$

Optimisation C is non-convex due to the rank one constraints[4], (19h), and line power constraints, (19c), which are of degree 4 w.r.t. the voltage vector variables $\boldsymbol{X}[t]$. The line power constraints can be brought into a linear form w.r.t. the voltage matrix variables $W[t]$ using Schur's complement formula [4], [29], allowing the constraints (19c) to be replaced by the Linear Matrix Inequality (LMI) constraints,

$$\begin{bmatrix} -\big(S_{lm}^{\max}\big)^2 & \mathrm{Tr}\{\boldsymbol{Y}_{lm} W[t]\} & \mathrm{Tr}\{\bar{\boldsymbol{Y}}_{lm} W[t]\} \\ \mathrm{Tr}\{\boldsymbol{Y}_{lm} W[t]\} & -1 & 0 \\ \mathrm{Tr}\{\bar{\boldsymbol{Y}}_{lm} W[t]\} & 0 & -1 \end{bmatrix} \preceq 0 \qquad \forall\, t \in \mathcal{T} \tag{20}$$

Removing the rank one constraints then yields a SDP, which is a convex problem. The convex SDP relaxation of the MOPF problem, Optimisation D, is therefore obtained from Optimisation C by using Schur's complement formula to replace the line power constraints, (19c), with the equivalent LMI constraints (20), and the removal of the rank one constraints, (19h).

[4] The set of rank one matrices in non-convex.

Optimisation D:

$$\min \quad \sum_n S_n \tag{21}$$

$$\text{over} \quad S_n, e_n[t], Q_{S,n}[t], W[t] \qquad \forall\, n, t$$

$$\text{subject to} \quad \mathrm{Tr}\{\boldsymbol{Y}_n W[t]\} \leq P_{G,n}[t] - P_{D,n}[t] - f_s(e_n[t] - e_n[t-1]) \tag{21a}$$

$$\mathrm{Tr}\{\bar{\boldsymbol{Y}}_n W[t]\} \leq Q_{G,n}[t] - Q_{D,n}[t] + Q_{S,n}[t] \tag{21b}$$

$$\begin{bmatrix} -\left(S_{lm}^{\max}\right)^2 & \mathrm{Tr}\{\boldsymbol{Y}_{lm} W[t]\} & \mathrm{Tr}\{\bar{\boldsymbol{Y}}_{lm} W[t]\} \\ \mathrm{Tr}\{\boldsymbol{Y}_{lm} W[t]\} & -1 & 0 \\ \mathrm{Tr}\{\bar{\boldsymbol{Y}}_{lm} W[t]\} & 0 & -1 \end{bmatrix} \preceq 0 \tag{21c}$$

$$(V_n^{\min})^2 \leq \mathrm{Tr}\{M_n W[t]\} \leq (V_n^{\max})^2 \tag{21d}$$

$$0 \leq e_n[t] \leq S_n \tag{21e}$$

$$S_n \geq 0 \tag{21f}$$

$$W[t] \succeq 0 \tag{21g}$$

$$\forall\, n \in \mathcal{N},\ (l,m) \in \mathcal{L},\ t \in \mathcal{T}$$

If the solution to this relaxation satisfies the rank one constraints of the original problem, then it is also a solution to the original, and therefore the solution obtained from the relaxation is exact.

The dual problem of Optimisation D, Optimisation E, is formulated by determining the Lagrangian of Optimisation D, $\mathscr{L}(\boldsymbol{x}, \boldsymbol{\lambda}, \boldsymbol{R}, \boldsymbol{\Omega})$, and then computing the dual cost function, $g(\boldsymbol{\lambda}, \boldsymbol{R}, \boldsymbol{\Omega})$, by minimising $\mathscr{L}$ w.r.t. the primal decision variables, collectively denoted $\boldsymbol{x}$, over the primal feasible region $\mathcal{S}$.

$$g(\boldsymbol{\lambda}, \boldsymbol{R}, \boldsymbol{\Omega}) = \inf_{\boldsymbol{x} \in \mathcal{S}} \mathscr{L}(\boldsymbol{x}, \boldsymbol{\lambda}, \boldsymbol{R}, \boldsymbol{\Omega}) \tag{22}$$

The dual problem is then the maximisation of the dual cost over the Lagrange multiplier dual variables, subject to appropriate constraints [27].

To produce the Lagrangian, the following Lagrange multipliers, dual decision variables, are defined:

1) $\lambda_{n,t}^P, \lambda_{n,t}^Q$: Lagrange multipliers associated with the slack real and reactive power conservations constraints, (21a) & (21b) respectively.
2) $\lambda_{n,t}^{VU}, \lambda_{n,t}^{VL}$: Lagrange multipliers associated with the upper and lower bound node voltage deviation constraints, (21d), respectively.
3) $\lambda_{n,t}^{eU}, \lambda_{n,t}^{eL}$: Lagrange multipliers associated with the upper and lower bound energy storage level consistency constraints, (21e), respectively.
4) λ_n^S: Lagrange multipliers associated with the non-negativity of storage capacity constraints, (21f).

5) $r^1_{(l,m),t}, r^2_{(l,m),t}, \ldots, r^6_{(l,m),t}$: The matrices,

$$R_{(l,m),t} = \begin{bmatrix} r^1_{(l,m),t} & r^2_{(l,m),t} & r^3_{(l,m),t} \\ r^2_{(l,m),t} & r^4_{(l,m),t} & r^5_{(l,m),t} \\ r^3_{(l,m),t} & r^5_{(l,m),t} & r^6_{(l,m),t} \end{bmatrix} \tag{23}$$

are the Lagrange multipliers associated with the line power constraint linear matrix inequalities, (21c).

6) The matrices $\Omega_t \in \mathbb{R}^{2N\times 2N}$ are the Lagrange multipliers associated with the positive semi-definiteness constraints on the matrix variables $W[t]$, (21g).

LMI constraints of form $A \preceq 0$, where A is symmetric, have corresponding symmetric Lagrange multipliers $Z \succeq 0$, and the constraint violation penalisation terms introduced into the Lagrangian are $\mathrm{Tr}\{AZ\}$ [27], and hence the corresponding complementary slackness KKT conditions are $\mathrm{Tr}\{AZ\} = 0$.

Using the Lagrange multipliers defined above, the Lagrangian of Optimisation D is produced.

Lagrangian of Optimisation D:

$$\begin{aligned}
\mathscr{L} = &\sum_n S_n \\
&+ \sum_{n,t} \lambda^P_{n,t} \left(\mathrm{Tr}\{\boldsymbol{Y}_n W[t]\} - P_{G,n}[t] + P_{D,n}[t] + f_s(e_n[t] - e_n[t-1]) \right) \\
&+ \sum_{n,t} \lambda^Q_{n,t} \left(\mathrm{Tr}\{\bar{\boldsymbol{Y}}_n W[t]\} - Q_{G,n}[t] + Q_{D,n}[t] - Q_{S,n}[t] \right) \\
&+ \sum_{(l,m),t} \left(-r^1_{(l,m),t}(S^{\max}_{lm})^2 + 2r^2_{(l,m),t}\,\mathrm{Tr}\{\boldsymbol{Y}_{lm} W[t]\} + 2r^3_{(l,m),t}\,\mathrm{Tr}\{\bar{\boldsymbol{Y}}_{lm} W[t]\} - r^4_{(l,m),t} - r^6_{(l,m),t} \right) \\
&+ \sum_{n,t} \left(\lambda^{VL}_{n,t} \left((V^{\min}_n)^2 - \mathrm{Tr}\{M_n W[t]\} \right) + \lambda^{VU}_{n,t} \left(\mathrm{Tr}\{M_n W[t]\} - (V^{\max}_n)^2 \right) \right) \\
&+ \sum_{n,t} \left(-\lambda^{eL}_{n,t} e_n[t] + \lambda^{eU}_{n,t}(e_n[t] - S_n) \right) \\
&+ \sum_n -\lambda^S_n S_n \\
&+ \sum_t \mathrm{Tr}\{\Omega_t(-W[t])\}
\end{aligned} \tag{24}$$

requiring,

$$\lambda^P_{n,t}, \lambda^Q_{n,t}, \lambda^{VU}_{n,t}, \lambda^{VL}_{n,t}, \lambda^{eU}_{n,t}, \lambda^{eL}_{n,t} \geq 0 \qquad \forall\, n \in \mathcal{N},\ t \in \mathcal{T} \tag{25a}$$

$$\lambda^S_n \geq 0 \qquad \forall\, n \in \mathcal{N} \tag{25b}$$

$$R_{(l,m),t} \succeq 0 \qquad \forall\, (l,m) \in \mathcal{L},\ t \in \mathcal{T} \tag{25c}$$

$$\Omega_t \succeq 0 \qquad \forall\, t \in \mathcal{T} \tag{25d}$$

and implicitly the satisfaction of the primal constraints, (21a-g).

Collecting terms yields,

$$\begin{aligned}\mathscr{L} =& \sum_n \left(1 - \lambda_n^S - \sum_t \lambda_{n,t}^{eU}\right) S_n \\ &+ \sum_{n,t} \Big(\mathrm{Tr}\{\lambda_{n,t}^P \boldsymbol{Y}_n W[t]\} + \mathrm{Tr}\{\lambda_{n,t}^Q \bar{\boldsymbol{Y}}_n W[t]\} - \mathrm{Tr}\{\lambda_{n,t}^{VL} M_n W[t]\} + \mathrm{Tr}\{\lambda_{n,t}^{VU} M_n W[t]\}\Big) \\ &+ \sum_{(l,m),t} \Big(\mathrm{Tr}\{2r_{(l,m),t}^2 \boldsymbol{Y}_{lm} W[t]\} + \mathrm{Tr}\{2r_{(l,m),t}^3 \bar{\boldsymbol{Y}}_{lm} W[t]\}\Big) \\ &+ \sum_{n,t} \Big(\lambda_{n,t}^P f_s(e_n[t] - e_n[t-1]) + (\lambda_{n,t}^{eU} - \lambda_{n,t}^{eL}) e_n[t]\Big) \\ &- \sum_{n,t} \Big(\lambda_{n,t}^Q Q_{S,n}[t]\Big) \\ &+ \sum_{n,t} \Big(\lambda_{n,t}^P (P_{D,n}[t] - P_{G,n}[t]) + \lambda_{n,t}^Q (Q_{D,n}[t] - Q_{G,n}[t]) + \lambda_{n,t}^{VL} (V_n^{\min})^2 - \lambda_{n,t}^{VU} (V_n^{\max})^2\Big) \\ &- \sum_{(l,m),t} \Big(r_{(l,m),t}^1 (S_{lm}^{\max})^2 + r_{(l,m),t}^4 + r_{(l,m),t}^6\Big) \\ &- \sum_t \big(\mathrm{Tr}\{\Omega_t W[t]\}\big)\end{aligned} \tag{26}$$

It is noted that the summation over the terms in the energy storage levels implicitly contains the initial states of charge via the dummy time instance, $e_n[t=0]$, introduced in Section III-B for notational compactness. However, as previously discussed, said initial charges are defined relative to the storage capacity primal decision variables S_n, as $e_n[0] = \alpha_n S_n$. Looking ahead to the minimisation of the Lagrangian, this dependence on S_n is introduced in an elegant way via the addition of a summation of zero terms, $e_n[0] - \alpha_n S_n = 0$,

$$\begin{aligned}\mathscr{L} =& \sum_n \left(1 - \lambda_n^S - \sum_t \lambda_{n,t}^{eU}\right) S_n \\ &+ \sum_{n,t} \Big(\mathrm{Tr}\{\lambda_{n,t}^P \boldsymbol{Y}_n W[t]\} + \mathrm{Tr}\{\lambda_{n,t}^Q \bar{\boldsymbol{Y}}_n W[t]\} - \mathrm{Tr}\{\lambda_{n,t}^{VL} M_n W[t]\} + \mathrm{Tr}\{\lambda_{n,t}^{VU} M_n W[t]\}\Big) \\ &+ \sum_{(l,m),t} \Big(\mathrm{Tr}\{2r_{(l,m),t}^2 \boldsymbol{Y}_{lm} W[t]\} + \mathrm{Tr}\{2r_{(l,m),t}^3 \bar{\boldsymbol{Y}}_{lm} W[t]\}\Big) \\ &+ \sum_{n,t} \Big(\lambda_{n,t}^P f_s(e_n[t] - e_n[t-1]) + (\lambda_{n,t}^{eU} - \lambda_{n,t}^{eL}) e_n[t]\Big) + \sum_n \Big(\lambda_{n,1}^P f_s(\underbrace{e_n[0] - \alpha_n S_n}_{0})\Big) \\ &- \sum_{n,t} \Big(\lambda_{n,t}^Q Q_{S,n}[t]\Big) \\ &+ \sum_{n,t} \Big(\lambda_{n,t}^P (P_{D,n}[t] - P_{G,n}[t]) + \lambda_{n,t}^Q (Q_{D,n}[t] - Q_{G,n}[t]) + \lambda_{n,t}^{VL} (V_n^{\min})^2 - \lambda_{n,t}^{VU} (V_n^{\max})^2\Big) \\ &- \sum_{(l,m),t} \Big(r_{(l,m),t}^1 (S_{lm}^{\max})^2 + r_{(l,m),t}^4 + r_{(l,m),t}^6\Big) \\ &- \sum_t \big(\mathrm{Tr}\{\Omega_t W[t]\}\big)\end{aligned} \tag{27}$$

Rearranging terms gives,

$$
\begin{aligned}
\mathscr{L} = & \sum_{n} \left(1 - \lambda_n^S - \alpha_n \lambda_{n,1}^P f_s - \sum_t \lambda_{n,t}^{eU}\right) S_n \\
& + \sum_{n,t} \Big(\mathrm{Tr}\{\lambda_{n,t}^P \boldsymbol{Y}_n W[t]\} + \mathrm{Tr}\{\lambda_{n,t}^Q \bar{\boldsymbol{Y}}_n W[t]\} - \mathrm{Tr}\{\lambda_{n,t}^{VL} M_n W[t]\} + \mathrm{Tr}\{\lambda_{n,t}^{VU} M_n W[t]\} \Big) \\
& + \sum_{(l,m),t} \Big(\mathrm{Tr}\{2 r_{(l,m),t}^2 \boldsymbol{Y}_{lm} W[t]\} + \mathrm{Tr}\{2 r_{(l,m),t}^3 \bar{\boldsymbol{Y}}_{lm} W[t]\} \Big) \\
& + \sum_{n,t} \Big(\lambda_{n,t}^P f_s (e_n[t] - e_n[t-1]) + (\lambda_{n,t}^{eU} - \lambda_{n,t}^{eL}) e_n[t] \Big) + \sum_n \Big(\lambda_{n,1}^P f_s e_n[0] \Big) \\
& - \sum_{n,t} \Big(\lambda_{n,t}^Q Q_{S,n}[t] \Big) \\
& + \sum_{n,t} \Big(\lambda_{n,t}^P (P_{D,n}[t] - P_{G,n}[t]) + \lambda_{n,t}^Q (Q_{D,n}[t] - Q_{G,n}[t]) + \lambda_{n,t}^{VL} (V_n^{\min})^2 - \lambda_{n,t}^{VU} (V_n^{\max})^2 \Big) \\
& - \sum_{(l,m),t} \Big(r_{(l,m),t}^1 (S_{lm}^{\max})^2 + r_{(l,m),t}^4 + r_{(l,m),t}^6 \Big) \\
& - \sum_t \big(\mathrm{Tr}\{\Omega_t W[t]\} \big)
\end{aligned}
\tag{28}
$$

At which point it is noticed that the remaining part of the introduced summation cancels with the trailing terms in $e_n[0]$ in the summation over terms in $e_n[t]$.

Finally, the matrix trace terms are brought together by noting that $\mathrm{Tr}\{AX\} + \mathrm{Tr}\{BX\} = \mathrm{Tr}\{AX + BX\} = \mathrm{Tr}\{(A+B)X\}$, resulting in,

$$\begin{aligned}
\mathscr{L} = &\sum_n \left(1 - \lambda_n^S - \alpha_n \lambda_{n,1}^P f_s - \sum_t \lambda_{n,t}^{eU}\right) S_n \\
&+ \sum_t \mathrm{Tr}\left\{\left(\sum_n \left(\lambda_{n,t}^P \boldsymbol{Y}_n + \lambda_{n,t}^Q \bar{\boldsymbol{Y}}_n - \lambda_{n,t}^{VL} M_n + \lambda_{n,t}^{VU} M_n\right)\right.\right. \\
&\qquad\qquad \left.\left. + \sum_{(l,m)} \left(2r_{(l,m),t}^2 \boldsymbol{Y}_{lm} + 2r_{(l,m),t}^3 \bar{\boldsymbol{Y}}_{lm}\right)\right) W[t]\right\} \\
&+ \sum_{n,t} \left(\lambda_{n,t}^P f_s (e_n[t] - e_n[t-1]) + (\lambda_{n,t}^{eU} - \lambda_{n,t}^{eL}) e_n[t]\right) + \sum_n \left(\lambda_{n,1}^P f_s e_n[0]\right) \\
&- \sum_{n,t} \left(\lambda_{n,t}^Q Q_{S,n}[t]\right) \\
&+ \sum_{n,t} \left(\lambda_{n,t}^P (P_{D,n}[t] - P_{G,n}[t]) + \lambda_{n,t}^Q (Q_{D,n}[t] - Q_{G,n}[t]) + \lambda_{n,t}^{VL} (V_n^{\min})^2 - \lambda_{n,t}^{VU} (V_n^{\max})^2\right) \\
&- \sum_{(l,m),t} \left(r_{(l,m),t}^1 (S_{lm}^{\max})^2 + r_{(l,m),t}^4 + r_{(l,m),t}^6\right) \\
&- \sum_t \left(\mathrm{Tr}\{\Omega_t W[t]\}\right)
\end{aligned} \tag{29}$$

Lagrangian Minimisation:

The dual cost function is determined by minimising[5] the Lagrangian derived w.r.t. the primal decisions variables, $\boldsymbol{x} = \{S_n, e_n[t], Q_{S,n}[t], W[t]\}_{n,t}$.

For the scalar primal variables $\{S_n, e_n[t], Q_{S,n}[t]\}$ this is performed by applying first order conditions to the Lagrangian [5], i.e. the set of stationarity KKT conditions for optimality [27].

$$\frac{\partial \mathscr{L}}{\partial S_n} = 1 - \lambda_n^S - \alpha_n \lambda_{n,1}^P f_s - \sum_t \lambda_{n,t}^{eU} = 0 \qquad \forall\, n \in \mathcal{N} \tag{30a}$$

$$\frac{\partial \mathscr{L}}{\partial e_n[t]} = f_s \left(\lambda_{n,t}^P - \lambda_{n,t+1}^P\right) + \left(\lambda_{n,t}^{eU} - \lambda_{n,t}^{eL}\right) = 0 \qquad \forall\, n \in \mathcal{N},\, t \in \mathcal{T} \backslash T \tag{30b}$$

$$\frac{\partial \mathscr{L}}{\partial e_n[T]} = f_s \lambda_{n,T}^P + \left(\lambda_{n,T}^{eU} - \lambda_{n,T}^{eL}\right) = 0 \qquad \forall\, n \in \mathcal{N} \tag{30c}$$

$$\frac{\partial \mathscr{L}}{\partial Q_{S,n}[t]} = -\lambda_{n,t}^Q = 0 \qquad \forall\, n \in \mathcal{N},\, t \in \mathcal{T} \tag{30d}$$

[5] Strictly determining the infimum of.

The equality $\lambda^{Q}_{n,t} = 0$ is expected, as sufficient reactive power support is assumed at all nodes, i.e. $Q_{S,n}[t]$ is unconstrained, and is un-penalised in the cost function. This causes the reactive power terms to not act in the optimisation, which can be interpreted as perfect local power factor correction at all buses in the network. This assumption is relaxed in Section VI-A, and reactive power information introduced to the optimisation problem.

Minimisation of $\mathscr{L}$ w.r.t. the primal matrix variables $W[t]$ relies on the following matrix trace inequality [30].

For positive semi-definite matrices $A, B \succeq 0$,

$$\lambda_{\min}(A)\,\mathrm{Tr}\{B\} \leq \mathrm{Tr}\{AB\} \leq \lambda_{\max}(A)\,\mathrm{Tr}\{B\} \tag{31}$$

where $\lambda_{\min}(A)\,, \lambda_{\max}(A)$ are the minimum and maximum eigenvalues of A respectively. Noting that for symmetric A, B, all eigenvalues are non-negative.

Therefore, if A, B symmetric and $\lambda_{\min}(A) = 0, \implies \mathrm{Tr}\{AB\} \geq 0$. Thus $\mathrm{Tr}\{AB\}$ has an achievable minimum of zero.

Define the following matrices,

$$\begin{aligned} A(\boldsymbol{\lambda}, \boldsymbol{R}, t) = &\sum_{n} \left(\lambda^{P}_{n,t}\boldsymbol{Y}_n + \lambda^{Q}_{n,t}\bar{\boldsymbol{Y}}_n + (\lambda^{VU}_{n,t} - \lambda^{VL}_{n,t})M_n\right) \\ &+ \sum_{(l,m)} \left(2r^{2}_{(l,m),t}\boldsymbol{Y}_{lm} + 2r^{3}_{(l,m),t}\bar{\boldsymbol{Y}}_{lm}\right) \qquad \forall\, t \in \mathcal{T} \end{aligned} \tag{32}$$

Considering the above mathematical result, and noting that as $A(\boldsymbol{\lambda}, \boldsymbol{R}, t)$ is a sum of symmetric matrices it is itself symmetric, it can be seen that the terms,

$$\mathrm{Tr}\{A(\boldsymbol{\lambda}, \boldsymbol{R}, t)W[t]\} \tag{33a}$$

$$\mathrm{Tr}\{\Omega_t W[t]\} \tag{33b}$$

can be minimised to zero provided,

$$A(\boldsymbol{\lambda}, \boldsymbol{R}, t) \succeq 0 \tag{34a}$$

$$\lambda_{\min}\big(A(\boldsymbol{\lambda}, \boldsymbol{R}, t)\big) = 0 \tag{34b}$$

$$\lambda_{\min}(\Omega_t) = 0 \tag{34c}$$

as $W[t] \succeq 0$ under the primal constraints (21g), and $\Omega_t \succeq 0$ under the dual constraints (25d).

Thus the terms in $\mathscr{L}$ in the primal matrix variables $W[t]$ can be minimised to zero by appropriate choices of the matrices $A(\boldsymbol{\lambda}, \boldsymbol{R}, t)$ and Ω_t.

As the choice of $\Omega_t \succeq 0$ is otherwise unconstrained, this variable is eliminated from the optimisation in the minimisation of $\mathscr{L}$. In fact $\Omega_t = 0$ satisfies the necessary and sufficient conditions for minimisation of $\mathscr{L}$.

In order for a non-infinite minimum of the trace terms in $A(\boldsymbol{\lambda}, \boldsymbol{R}, t)$ to exist, specifically a zero minimum, the following constraints are introduced to the dual problem,

$$\sum_{n}\Big(\lambda^{P}_{n,t}\boldsymbol{Y}_n+\lambda^{Q}_{n,t}\bar{\boldsymbol{Y}}_n+(\lambda^{VU}_{n,t}-\lambda^{VL}_{n,t})M_n\Big)+\sum_{(l,m)}\Big(2r^{2}_{(l,m),t}\boldsymbol{Y}_{lm}+2r^{3}_{(l,m),t}\bar{\boldsymbol{Y}}_{lm}\Big)\succeq 0 \qquad \forall\, t\in\mathcal{T} \tag{35}$$

The necessary conditions $\lambda_{\min}\big(A(\boldsymbol{\lambda},\boldsymbol{R},t)\big)=0$ will be shown to be redundant in the proof of the conditions for exactness, and hence are omitted as constraints.

In light of the minimisations identified, (30) & (33), the dual cost is found to be,

$$\begin{aligned} g(\boldsymbol{\lambda},\boldsymbol{R},\boldsymbol{\Omega}) &= \inf_{\boldsymbol{x}\in\mathcal{S}}\mathscr{L}(\boldsymbol{x},\boldsymbol{\lambda},\boldsymbol{R},\boldsymbol{\Omega}) \\ &= \sum_{n,t}\Big(\lambda^{P}_{n,t}(P_{D,n}[t]-P_{G,n}[t])+\lambda^{Q}_{n,t}\cancelto{0}{(Q_{D,n}[t]-Q_{G,n}[t])}+\lambda^{VL}_{n,t}(V^{\min}_{n})^2-\lambda^{VU}_{n,t}(V^{\max}_{n})^2\Big) \\ &\quad-\sum_{(l,m),t}\Big(r^{1}_{(l,m),t}(S^{\max}_{lm})^2+r^{4}_{(l,m),t}+r^{6}_{(l,m),t}\Big) \end{aligned} \tag{36}$$

From this, and the necessary conditions/constraints identified previously, the dual problem, Optimisation E, is formulated.

Optimisation E - Dual Problem:

$$\begin{aligned} \max\quad & \sum_{n,t}\Big(\lambda^{P}_{n,t}(P_{D,n}[t]-P_{G,n}[t])+\lambda^{VL}_{n,t}(V^{\min}_{n})^2-\lambda^{VU}_{n,t}(V^{\max}_{n})^2\Big) \\ & \qquad-\sum_{(l,m),t}\Big(r^{1}_{(l,m),t}(S^{\max}_{lm})^2+r^{4}_{(l,m),t}+r^{6}_{(l,m),t}\Big) && (37)\\ \text{over}\quad & \lambda^{P}_{n,t},\lambda^{Q}_{n,t},\lambda^{VU}_{n,t},\lambda^{VL}_{n,t},\lambda^{eU}_{n,t},\lambda^{eL}_{n,t},\lambda^{S}_{n},R_{(l,m),t} \qquad \forall\, n,(l,m),t \\ \text{subject to}\quad & 1-\lambda^{S}_{n}-\alpha_n\lambda^{P}_{n,1}f_s-\sum_{t}\lambda^{eU}_{n,t}=0 && (37a)\\ & f_s\Big(\lambda^{P}_{n,t}-\lambda^{P}_{n,t+1}\Big)+\Big(\lambda^{eU}_{n,t}-\lambda^{eL}_{n,t}\Big)=0 && (37b)\\ & f_s\lambda^{P}_{n,T}+\Big(\lambda^{eU}_{n,T}-\lambda^{eL}_{n,T}\Big)=0 && (37c)\\ & \sum_{n}\Big(\lambda^{P}_{n,t}\boldsymbol{Y}_n+(\lambda^{VU}_{n,t}-\lambda^{VL}_{n,t})M_n\Big)+\sum_{(l,m)}\Big(2r^{2}_{(l,m),t}\boldsymbol{Y}_{lm}+2r^{3}_{(l,m),t}\bar{\boldsymbol{Y}}_{lm}\Big)\succeq 0 && (37d)\\ & \lambda^{P}_{n,t},\lambda^{Q}_{n,t},\lambda^{VU}_{n,t},\lambda^{VL}_{n,t},\lambda^{eU}_{n,t},\lambda^{eL}_{n,t},\lambda^{S}_{n}\geq 0 && (37e)\\ & R_{(l,m),t}\succeq 0 && (37f)\\ & \forall\, n\in\mathcal{N},\ (l,m)\in\mathcal{L},\ t\in\mathcal{T} \end{aligned}$$

Optimisation E is seen to consist of the maximisation of a linear objective function, subject to a combination of affine and LMI constraints on the decision variables, and is therefore a SDP, and thus convex.

C. Proof of Conditions for Exactness

Both Optimisations D & E are convex, hence strong duality can be shown to hold between them by the satisfaction of the weak form of Slater's condition [5].

(Weak) Slater's Condition [27]:

For a convex optimisation problem,

$$\begin{aligned} \min \quad & f_0(\boldsymbol{x}) \\ \text{subject to} \quad & f_i(\boldsymbol{x}) \leq 0 \quad i = 1, \ldots, m \\ & h_i(\boldsymbol{x}) = 0, \; i = 1, \ldots, p \end{aligned} \tag{38}$$

where $f_1, \ldots, f_k$ are affine. Strong duality holds, $d^* = p^*$, if there exists a partially strictly feasible solution to the primal problem, that is:

$$\begin{aligned} \exists \, \boldsymbol{x}_0 \in \text{relint}(\mathcal{D}) \; : \; & f_i(\boldsymbol{x}_0) \leq 0, \; i = 1, \ldots, k \\ & f_i(\boldsymbol{x}_0) < 0, \; i = k{+}1, \ldots, m \\ & h_i(\boldsymbol{x}_0) = 0, \; i = 1, \ldots, p \end{aligned} \tag{39}$$

The following thought experiment details a partially strictly feasible solution to the convex primal problem, Optimisation D, and by demonstrating satisfaction of Slater's condition shows that there is zero duality gap between Optimisations D & E.

Consider each node to have an infinity large storage capacity, i.e. S_n arbitrarily large $\forall \, n$, which satisfies the primal constraints $S_n \geq 0$, (21f). Assume that at all time instances, every node in the network operates at a constant voltage $\tilde{V}_n$ which satisfies $V_n^{\min} \leq \left|\tilde{V}_n\right| \leq V_n^{\max}$. By consideration of the underlying power transmission physics, no power flow occurs in the lines $\implies \text{Tr}\{\boldsymbol{Y}_n W[t]\} = \text{Tr}\{\bar{\boldsymbol{Y}}_n W[t]\} = \text{Tr}\{\boldsymbol{Y}_{lm} W[t]\} = \text{Tr}\{\bar{\boldsymbol{Y}}_{lm} W[t]\} = 0$. Therefore, the primal line power and node voltage constraints, (21c) & (21d), are satisfied, with the non-affine LMI constraint (21c) being strictly satisfied,

$$\begin{bmatrix} -\left(S_{lm}^{\max}\right)^2 & 0 & 0 \\ 0 & -1 & 0 \\ 0 & 0 & -1 \end{bmatrix} = - \begin{bmatrix} \left(\left(S_{lm}^{\max}\right)^2 - 1\right)^{1/2} \\ 0 \\ 0 \end{bmatrix} \begin{bmatrix} \left(\left(S_{lm}^{\max}\right)^2 - 1\right)^{1/2} \\ 0 \\ 0 \end{bmatrix}^T - I \prec 0 \tag{40}$$

As $W[t]$ is constructed as a vector outer-product, $W[t] = \tilde{\boldsymbol{V}} \tilde{\boldsymbol{V}}^T \; \forall \, t \in \mathcal{T}$, it is positive semi-definite, and so (21g) is satisfied.

Let the initial states of charge $e_n[0] < S_n$ be arbitrarily large. Consider at each time instance where a real power deficit occurs at a bus, sufficient energy being withdrawn from the local storage unit as to over-satisfy the demand deficit by an amount ε, which is dumped. At time instances where a surplus occurs, said surplus is curtailed. This results in the storage energy levels evolving as,

$$\frac{e_n[t] - e_n[t-1]}{\Delta t} = \begin{cases} (P_{G,n}[t] - P_{D,n}[t]) - \varepsilon & \text{for } P_{G,n}[t] - P_{D,n}[t] \leq 0 \\ 0 & \text{for } P_{G,n}[t] - P_{D,n}[t] > 0 \end{cases} \tag{41}$$

Under this operation scheme, $e_n[t]$ is a weakly decreasing series, however, as it starts at an arbitrarily large energy level, and the time horizon T and power deficits $P_{G,n}[t] - P_{D,n}[t] \leq 0$ are finite, $e_n[T] > 0$ is satisfied, as $e_n[0] > (\max_t(P_{D,n}[t]) + \varepsilon)T \ \forall\, n$ by construction. As $Q_{S,n}[t]$ is unconstrained, it can be chosen to provide a reactive power surplus in all time instances. Therefore, the primal real and reactive slack power conservation constraints, (21a) & (21b), and energy level consistency constraints, (21e), are also strictly satisfied.

As such, a partially strictly feasible solution to the primal problem has been constructed, and in doing so the weak form of Slater's condition satisfied.

A strictly feasible solution to the dual problem can be constructed by selecting the values of the Lagrange multipliers appropriately, following a similar procedure as in [5],

$$\lambda_n^S = 1 \ , \ \lambda_{n,t}^P = 0 \ , \ \lambda_{n,t}^{eU} = \lambda_{n,t}^{eL} = 0 \ , \ \lambda_{n,t}^{VU} = 2 \ , \ \lambda_{n,t}^{VL} = 1 \ , \ R_{(l,m),t} = I \qquad (42)$$

noting that $\sum_k M_k = I$.

Therefore strong duality holds between Optimisation D and Optimisation E.

Extension of Proof of Single Period Condition for Exactness:

Reference [4] proves the following conditions for exactness of the SDP relaxation dual, "*Theorem 2*: The following statements hold:

1) The duality gap is zero for Optimization 1 if and only if the SDP Optimization 3 has a rank-one solution W^{opt}.
2) The duality gap is zero for Optimization 1 if its dual (i.e. the SDP Optimization 4) has a solution $(x^{\text{opt}}, r^{\text{opt}})$ such that the positive semidefinite matrix $A(x^{\text{opt}}, r^{\text{opt}})$ has a zero eigenvalue of multiplicity 2."

Condition 1) is proved simply by noting that, if the optimal value of the voltage matrix variable, W^{opt}, is rank one, then the optimal solution to Optimization 3 satisfies the rank one constraint of Optimization 2. Hence, said optimal solution is in the feasible region of Optimization 2 and so optimal for the unrelaxed problem, which has been shown to be equivalent to the original problem.

This condition for exactness is trivial to extend to the multi-period case by noting that, if the SDP Optimisation D, (21), has an optimal solution which consists of a sequence of rank one voltage matrices, $\{W^{\text{opt}}[t]\}_{t=1}^T$, then said optimal solution satisfies the rank one constraints of the unrelaxed problem Optimisation C, (19). Therefore, it is optimal for the unrelaxed problem, and thus by the equivalence of Optimisations C & A, is the optimal solution to the original MOPF problem, Optimisation A, (12).

The proof of Condition 2) in [4] proceeds through the consideration of the following KKT condition for optimality of Optimization 4,

$$\text{Tr}\{A(x^{\text{opt}}, r^{\text{opt}})W^{\text{opt}}\} = 0 \qquad (43)$$

By consideration of this condition, and the positive semi-definiteness of the two matrices, it is shown that the eigenvectors of W^{opt} corresponding to non-zero eigenvalues all belong to the null space of $A(x^{\text{opt}}, r^{\text{opt}})$. If $A(x^{\text{opt}}, r^{\text{opt}})$ has a zero eigenvalue of multiplicity two, resulting in a null space of dimension two, then non-zero W^{opt} must have $f \in \{1, 2\}$ non-zero eigenvalues. When $f = 1$, W^{opt} is rank one, and hence as before the solution to the

dual problem is exact. When $f = 2$, it can be shown that there exists a rank one solution to Optimization 3, which is constructed from the vectors spanning the null space of $A(x^{\text{opt}}, r^{\text{opt}})$, and hence this solution to Optimization 3 is exact.

The condition on the dimension of the null space of A for achieving zero duality gap is extended to the multi-period case, by noting that the procedure for the minimisation of the Lagrangian of Optimisation D w.r.t. the voltage matrix variables to produce the dual cost, developed an equivalent set of KKT conditions for optimality of the dual problem solution,

$$\text{Tr}\left\{A(\boldsymbol{\lambda}^{\text{opt}}, \boldsymbol{R}^{\text{opt}}, t)W^{\text{opt}}[t]\right\} = 0 \qquad \forall\, t \in \mathcal{T} \tag{44}$$

These KKT conditions are the basis of an analogous proof in reference [5]. It is noted that all matrices $A(\boldsymbol{\lambda}^{\text{opt}}, \boldsymbol{R}^{\text{opt}}, t)$, defined in (32), are composed of independent sets of Lagrange multipliers, and therefore, the trace KKT conditions must be satisfied independently at all time instances at the optimal solution.

As the KKT conditions are separable in the time instances, the proof of the existence of a rank one solution matrix $W^{\text{opt}}[t]$ when the corresponding multiplier matrix, $A(\boldsymbol{\lambda}^{\text{opt}}, \boldsymbol{R}^{\text{opt}}, t)$, has a null space of dimension two, can be applied independently to all time instances. Thus, if all time instances have A-matrices with null spaces of dimension two, then there exists a sequence of rank one voltage matrices which form a solution to Optimisation D[6]. Hence, as before, said solution attains zero duality gap, i.e. is exact.

It is noted that satisfaction of the null space conditions on the A-matrices is sufficient for satisfaction of the necessary eigenvalue conditions for optimality, (34b).

Therefore, the following equivalent statements for the exactness of the multi-period problem have been proved:

1) The duality gap is zero for Optimisation A if and only if the SDP Optimisation D has a solution consisting of a sequence of rank one voltage matrices, $\{W^{\text{opt}}[t]\}_{t=1}^{T}$.
2) The duality gap is zero for Optimisation A if its dual (i.e. the SDP Optimisation E) has a solution $(\boldsymbol{\lambda}^{\text{opt}}, \boldsymbol{R}^{\text{opt}})$ such that the positive semi-definite matrices $\{A(\boldsymbol{\lambda}^{\text{opt}}, \boldsymbol{R}^{\text{opt}}, t)\}_{t=1}^{T}$ all have zero eigenvalues of multiplicity 2.

These exactness conditions are both necessary and sufficient [4].

D. Solution Strategy & System Operation Recovery

The proofs in Section IV-C show that, provided the exactness conditions are satisfied, it is possible to determine the optimal solution to the original MOPF problem, Optimisation A, from the solution to the convex SDP dual problem, Optimisation E. This section details the computational procedure required to recover a solution to the original MOPF problem, initially for exact dual solutions where the necessary and sufficient conditions for zero duality gap are satisfied, and subsequently for attempts to recover an approximate solution when said conditions fail.

[6] That the optimal solution to the dual problem, Optimisation E, yields an optimal solution to the SDP relaxation, Optimisation D, follows from exactness of the dual solution. Strong duality between the two problems was proved via the satisfaction of Slater's condition.

Solution Recovery Under Exactness Conditions:

Assuming that Optimisation E, (37), is feasible and every feasible solution is non-trivial, i.e. satisfies $W[t] \neq 0,\ \forall\, t \in \mathcal{T}$, and that the optimal solution found when solved satisfies the exactness conditions outlined above[7]; the solution to Optimisation A is determined by the following procedure [5]:

1) Solve Optimisation E and verify that it yields a feasible solution which satisfies the conditions for exactness.
2) For each $t \in \mathcal{T}$:
   i) Find any non-zero vector $[v_1[t]^T\, v_2[t]^T]^T$ in the null space of $A(\boldsymbol{\lambda}^{\text{opt}}, \boldsymbol{R}^{\text{opt}}, t)$, where $v_1[t], v_2[t] \in \mathbb{R}^N$.
   ii) Compute the optimal node voltage vector $\boldsymbol{V}[t]^{\text{opt}}$ as,
   $$\boldsymbol{V}[t]^{\text{opt}} = (\zeta_1[t] + \zeta_2[t]\mathbf{j})(v_1[t] + v_2[t]\mathbf{j}) \tag{45}$$
   where the real, scalar constants $\zeta_1[t], \zeta_2[t]$ are determined from the complementary slackness KKT conditions,
   $$\lambda^{VL}_{n,t}\left((V^{\min}_n)^2 - \left|V_n[t]^{\text{opt}}\right|^2\right) = 0 \tag{46a}$$
   $$\lambda^{VU}_{n,t}\left(\left|V_n[t]^{\text{opt}}\right|^2 - (V^{\max}_n)^2\right) = 0 \tag{46b}$$
   and the known complex voltage of the reference bus. See Appendix I-A for details on solving these equations.
   iii) Convert the determined $\boldsymbol{V}[t]^{\text{opt}}$ to the expanded voltage vector $\boldsymbol{X}[t]^{\text{opt}}$, and from this compute $W[t]^{\text{opt}} = \boldsymbol{X}[t]^{\text{opt}}(\boldsymbol{X}[t]^{\text{opt}})^T$
3) Compute the optimal values of the primal decision variables by solving the complementary slackness KKT conditions,
   $$\lambda^{P}_{n,t}\left(\text{Tr}\{\mathbf{Y}_n W[t]\} - P_{G,n}[t] + P_{D,n}[t] + f_s(e_n[t] - e_n[t-1])\right) = 0 \tag{47a}$$
   $$\lambda^{Q}_{n,t}\left(\text{Tr}\{\bar{\mathbf{Y}}_n W[t]\} - Q_{G,n}[t] + Q_{D,n}[t] - Q_{S,n}[t]\right) = 0 \tag{47b}$$
   $$-\lambda^{eL}_{n,t} e_n[t] = 0 \tag{47c}$$
   $$\lambda^{eU}_{n,t}(e_n[t] - S_n) = 0 \tag{47d}$$
   $$-\lambda^{S}_{n} S_n = 0 \tag{47e}$$
   $$\forall\, n \in \mathcal{N},\ t \in \mathcal{T}$$
   Appendix I-B provides a computationally efficient method of reconstructing $\{e_n[t]\}_{n,t}$ and $\{S_n\}_n$ from these KKT conditions.

The recovered optimal values of the primal decision variables provide complete information about both the optimal energy storage infrastructure development strategy, $\{S^*_n\}^N_{n=1}$, and the optimal system operation strategy, $\{e^*_n[t]\}_{n,t}$, over the time window $\mathcal{T}$. Additionally, considering the price interpretation of Lagrange multipliers, the optimal Lagrange multiplier values provide information on the optimal energy pricing strategies for network operation.

[7] Note that this condition can only be verified once the optimal solution to the dual problem, (37), has been determined.

Primal Domain Solution Recovery for Non-Exact Time Instances:

When the dual problem is solved, and the null space condition on $A(\boldsymbol{\lambda}^{\text{opt}}, \boldsymbol{R}^{\text{opt}}, t)$ is found to not be satisfied by some subset of the time instances in the observation window, for these time instances the solution recovery procedure from [5] cannot be used, as it requires the null space to have dimension two in order to derive (45). See proof of Corollary 1 in [4]. Further, as the conditions for exactness are both necessary and sufficient, this implies that if any time instance does not satisfy the null space condition, then the duality gap between Optimisations A & E is non-zero. Additionally, as exactness of the relaxation dual solution requires the existence of a sequence of rank one optimal voltage matrices, any non-exact solution cannot satisfy the rank one constraints of Optimisation C, (19h), and thus cannot be feasible w.r.t. the original problem.

However, the duality gap may be small for such non-exact solutions, and if a primal domain solution[8] can be recovered, it may provide valuable information on near optimal system development and operation strategies, i.e. an approximate solution to the original problem, Optimisation A.

The proposed recovery method seeks to identify voltage matrices of minimum rank which satisfy the enforceable primal domain constraints, and the KKT necessary conditions for optimality (44). In doing so it is hoped to recover voltage matrices which are primal feasible, and as close as possible to the exact solution in rank terms. This recovery method therefore takes the form of an optimisation problem.

The primal domain constraints (21a) & (21b) are not enforceable at the time of voltage matrix recovery, as the energy levels $e_n[t]$ are unknown. Therefore the remaining primal constraints on $W[t]$, (21c) & (21d), are used.

This leads to the recovery optimisation for each non-exact time instance,
$t \in \{\mathcal{T} : \text{rank}(A(\boldsymbol{\lambda}^{\text{opt}}, \boldsymbol{R}^{\text{opt}}, t)) < 2N-2\}$,

$$
\begin{aligned}
\min \quad & \text{rank}(W[t]) && (48)\\
\text{over} \quad & W[t] \\
\text{subject to} \quad & \text{Tr}\left\{A(\boldsymbol{\lambda}^{\text{opt}}, \boldsymbol{R}^{\text{opt}}, t)W[t]\right\} = 0 && (48a)\\
& \begin{bmatrix} -\left(S_{lm}^{\max}\right)^2 & \text{Tr}\{\boldsymbol{Y}_{lm}W[t]\} & \text{Tr}\{\bar{\boldsymbol{Y}}_{lm}W[t]\} \\ \text{Tr}\{\boldsymbol{Y}_{lm}W[t]\} & -1 & 0 \\ \text{Tr}\{\bar{\boldsymbol{Y}}_{lm}W[t]\} & 0 & -1 \end{bmatrix} \preceq 0 && (48b)\\
& (V_n^{\min})^2 \leq \text{Tr}\{M_n W[t]\} \leq (V_n^{\max})^2 && (48c)\\
& W[t] \succeq 0 && (48d)\\
& \forall\, n \in \mathcal{N},\ (l,m) \in \mathcal{L}
\end{aligned}
$$

However, this optimisation problem is non-convex due to the rank objective, and therefore intractable to solve - it is known to be NP-hard [31]. To achieve a computationally feasible recovery method, a convex relaxation of the rank minimisation problem is produced using a Nuclear-norm objective [31], resulting in the relaxation optimisation,

[8] Note, the voltage solution matrices being of rank not equal to one precludes the existence of corresponding voltage vectors, and hence the solution can only be feasible w.r.t. the domain of Optimisation D.

$$\min \quad \sum_{i=1}^{2N} \sigma_i \left(W[t]\right) \tag{49}$$

$$\text{over} \quad W[t]$$

$$\text{subject to} \quad \mathrm{Tr}\left\{A(\boldsymbol{\lambda}^{\text{opt}}, \boldsymbol{R}^{\text{opt}}, t) W[t]\right\} = 0 \tag{49a}$$

$$\begin{bmatrix} -\left(S_{lm}^{\max}\right)^2 & \mathrm{Tr}\{\boldsymbol{Y}_{lm} W[t]\} & \mathrm{Tr}\{\bar{\boldsymbol{Y}}_{lm} W[t]\} \\ \mathrm{Tr}\{\boldsymbol{Y}_{lm} W[t]\} & -1 & 0 \\ \mathrm{Tr}\{\bar{\boldsymbol{Y}}_{lm} W[t]\} & 0 & -1 \end{bmatrix} \preceq 0 \tag{49b}$$

$$(V_n^{\min})^2 \leq \mathrm{Tr}\{M_n W[t]\} \leq (V_n^{\max})^2 \tag{49c}$$

$$W[t] \succeq 0 \tag{49d}$$

$$\forall\, n \in \mathcal{N},\ (l,m) \in \mathcal{L}$$

Where $\sigma_i\left(W[t]\right)$ is the i^{th} singular value of $W[t]$. This optimisation can be seen to be a convex SDP.

Once the voltage matrices $W[t]$ have been recovered, the procedure in Appendix I-B is then used to recover energy level and storage capacity information, and in doing so construct the remainder of the primal feasible approximate solution.

E. Problem Characteristics

The optimisation formulation, Section IV-B, and subsequent proof of conditions for exactness, Section IV-C, demonstrate that an optimal solution to the original MOPF problem, Optimisation A, can be determined by solving a convex SDP, Optimisation E, provided the dual solution satisfies the conditions for exactness. There exist efficient algorithms for solving SDP/LMI problems, which have been shown to have polynomial time complexity [32], and the convexity of the problem provides both computational and solution accuracy guarantees. Further, the dual problem of a SDP is itself a SDP, and strong duality often holds [4], [33]. This motivates the formulation employed, as it provides a pathway for solving the NP-hard original problem [4] in a convex manner, with the dual problem being exact, and exploited to provide a method for numerically determining rank one solution matrices $W[t]$. The problem cannot be solved directly from Optimisation D, as if a rank one solution exists, then infinitely many rank two solutions exist [4], hence the rank one solution cannot be recovered.

Observing Optimisation E, it can be seen that the optimisation involves $N+6NT+12LT \rightarrow O((N+L)T)$ decision variables, where N is the number of nodes, and L the number of lines. As power transmission networks are typically very sparse, $\implies L \approx N$, and thus the dimension of the problem reduces to $O(NT)$. Given a fixed network for study, i.e. fixed N, the dimension of the problem then only increases linearly with the observation duration T, which is an attractive property of the formulation.

As illustrated in Fig. 4, the dual problem has a structure which is 'super sparse' in time, with the constraint sets being almost completely de-coupled between time instances, linked only to adjacent sets via the real power conservation constraint Lagrange multipliers, $\lambda_{n,t}^{P}$. This property of the problem may be able to be exploited by a dedicated solver algorithm to provide low computational complexity in T, and thus yield an extremely computationally

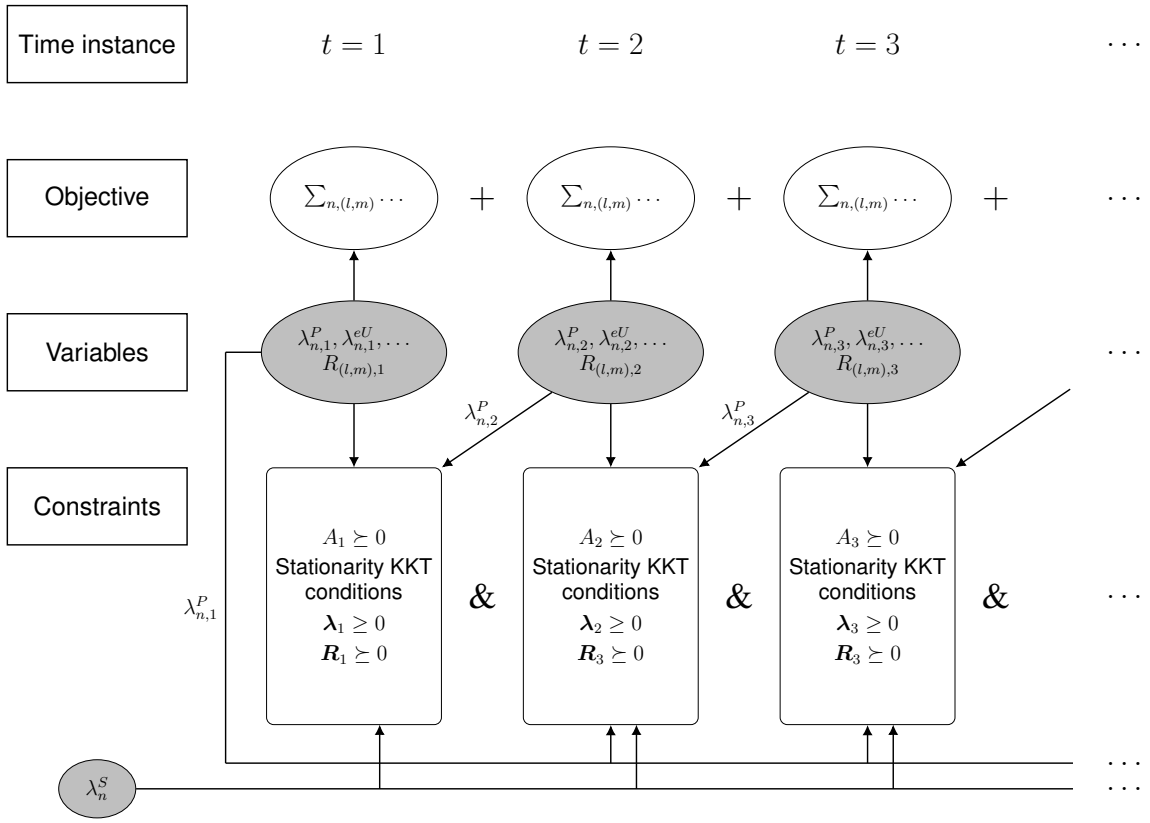

Fig. 4: Sparse structure of dual problem, Optimisation E, (37)

efficient solution strategy. However, in the network size dimension, N, the problem is 'dense', and hence may scale poorly for large networks, with high computational complexity in N. This may make the method unsuited to the analysis of large-scale networks, such as the SciGRID [34] or GridKit [35] European transmission network models commonly used in literature [1], [36].

Considering the derivation of the aggregate Lagrange multiplier matrices $A(\boldsymbol{\lambda}, \boldsymbol{R}, t)$ corresponding to the voltage matrices $W[t]$, given by (32), it can be seen that their value is unaffected by the addition of energy storage dynamics to the OPF problem. Hence, as stated in [5], "adding affine charge/discharge dynamics to the OPF problem does not change the structure of the dual variable that provides the basis for the main result in [4], [6]". Indeed, the addition of any further affine dynamics to the MOPF problem does not alter the structure of the dual variables $A(\boldsymbol{\lambda}, \boldsymbol{R}, t)$, and retains the conditions for exactness. In this way, the optimisation can be extended to model any further aspects of power systems behaviour which can be described by affine constraints, whilst maintaining the convexity and exactness properties of the formulation.

V. Numerical Results

A. Experimental Methodology

A Python-based implementation of the solution strategy described in Section IV-D was developed, code listings for which are available in the online appendix. The solver libraries CVXOPT [37], [38] & SCS [39], [40], interfaced via CVXPY [41], [42], were used for solving the dual problem, (37), and non-exact voltage matrix recovery problem, (49), respectively.

Numerical experiments were carried out to test the validity of the optimisation method developed. These tests were performed on a simplified model of the UK transmission level power system [43], shown in Fig. 1, assuming a nominal $400kV$ bus voltage, and a typical $(25 + \mathbf{j}210)m\Omega/km$ line impedance [44], [45]. Hourly power generation data for both wind and solar at each bus was synthesised from historic meteorological observation data, obtained from the MetOffice MIDAS dataset [11], and appropriate technology models [12], [13]. Hourly resolved power demand data was obtained from the GridWatch dataset [46]. The complete data preparation methodology is available in the online appendix.

In each test, the dual optimisation was performed for a given time window within the historic observation period, satisfaction of the conditions for exactness checked for the solution obtained, and a primal domain solution recovery attempted.

B. Satisfaction of Exactness Conditions

The numerical experiments demonstrated that in many instances the conditions for exactness of the dual problem were satisfied by the UK power transmission network, and hence that the optimisation method was able to determine a solution to the original renewable power system optimisation problem via a convex formulation. Thus, it was demonstrated that the UK power grid topology is amenable to the studied class of SDP relaxation dual formulations for MOPF problems.

The importance of this demonstration of exactness is compounded by the result from Section IV-B of [4], which proves[9]that, "[For general networks with no reactive-load constraints,] when the duality gap is zero for a topology Y, then the ε-modified problem corresponding to every possible [set of] load profiles and physical limits can be convexified".

The ε-modified problem is the dual problem, (37), subject to the additional constraints,

$$\|\boldsymbol{\lambda}_t\| \leq \frac{1}{\varepsilon} \ , \ \|\boldsymbol{r}_t\| \leq \frac{1}{\varepsilon} \ , \ \varepsilon \leq \lambda^P_{n,t} \leq \frac{1}{\varepsilon} \qquad \forall\, n \in \mathcal{N},\, t \in \mathcal{T} \tag{50}$$

for some small $\varepsilon > 0$, which corresponds to the dual of a perturbed version of the modified MOPF problem [4].

This result proves the existence of a reliable method for determining arbitrarily accurate approximations to MOPF problems on this topology via a convex method, guaranteeing the determination of the global optimum in polynomial time. The solution is obtained by solving the convex ε-modified problem, which is both guaranteed to be exact, and shown to achieve the same solution as the original [4].

Table I and Fig. 5 illustrate the exact solution obtained from the optimisation over the time window `2018-03-01 9:00` $\rightarrow$ `2018-03-01 21:00`. The solution indicates that, for operation over this time window, there is a subset of nodes at which it is most beneficial to locate energy storage. However, as this observation duration is only 12 hours, limited insight that can be gained into the optimal placement strategy for long-term behaviour of the system, and the solution is provided for purely illustrative purposes.

[9] The extension of the proof to the multi-period case follows from the separability of the matrices $A(\boldsymbol{\lambda}, \boldsymbol{R}, t)$ in time, as with the extension of the proof of conditions for exactness.

Bus, n	1	2	3	4	5	6	7	8	9	10
S_n^{opt} (MWh)	66,963	392	71,328	9,062	64,902	1,596	450	0	0	9

TABLE I: Optimal bus storage capacities of exact solution to time window `2018-03-01 9:00` → `2018-03-01 21:00`

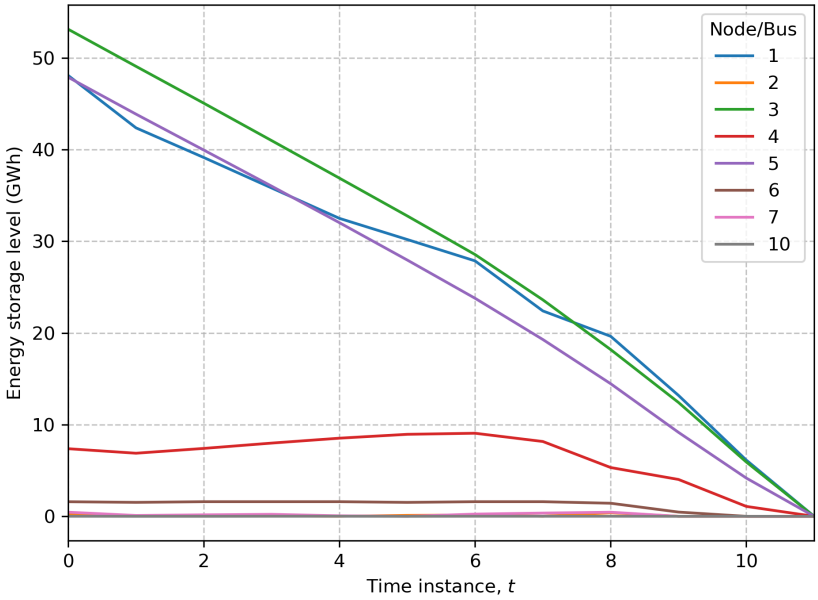

Fig. 5: Recovered energy levels of exact solution to time window `2018-03-01 9:00` → `2018-03-01 21:00`

C. *Performance of Non-Exact Solution Recovery*

During experimentation, it was found that for a number of time windows, the optimal solution to the dual problem failed to satisfy the conditions for exactness. When the non-exact voltage matrix recovery method presented in Section IV-D was performed on these time instances, it achieved rather limited results, with the solutions to the optimisation yielding either full rank or very high rank matrices, and in some instances violating the positive semi-definiteness constraints, (49d). Further, the energy level recovery methods described in Appendix I-B were sometimes found to yield profiles which were either infeasible or inconsistent with the optimised dual objective.

Tables II & III and Fig. 6 detail the approximate solutions obtained by the two energy level recovery methods for the non-exact observation period `2018-03-01 9:00` → `2018-04-01 09:00`. It can be seen that the energy levels recovered by the KKT, complementary slackness based method are infeasible, thus invalidating the corresponding total storage capacity value, whilst the robust, global consistency method provides a poor fit to the optimised dual objective.

The results of the experiments suggest that, where the conditions for exactness are not satisfied, the proposed solution recovery methods cannot provide a good reconstruction of the near optimal behaviour of the power system, and hence, the approximate solution to the optimal storage distribution problem can neither be determined nor validated. Thus, a deeper understanding of the factors determining solution exactness is required for the formulation to be confidently utilised on arbitrary power profiles.

Bus, n		1	2	3	4	5	6	7	8	9	10
S_n^{opt} (GWh)	KKT	75.7	4.2	133.0	10.8	69.6	2.0	0.9	0.2	0.1	0.2
	Robust	76.5	11.2	133.0	10.9	80.2	6.0	14.1	89.5	0.2	0.4

TABLE II: Comparison of non-exact recovery method storage capacity estimates

Method	Dual objective, d^*	KKT recovery	'Robust' recovery
$\sum_n S_n^{\text{opt}}$ (GWh)	295.4	296.7	422.0
% difference	–	+0.442	+42.9

TABLE III: Comparison of non-exact recovery method objective values

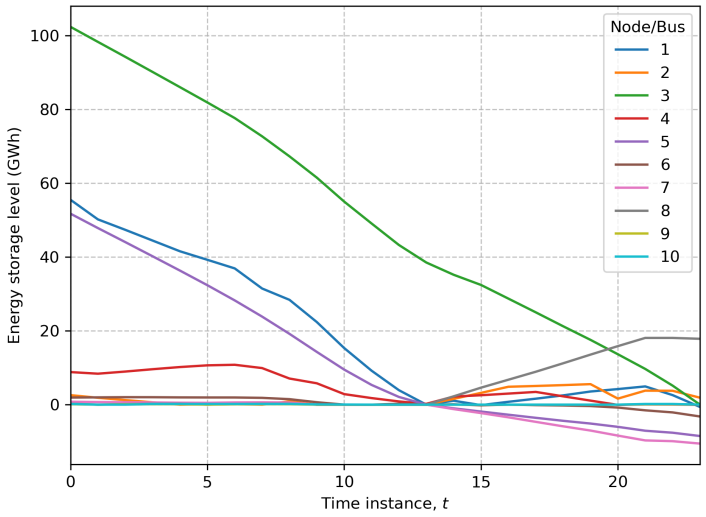

(a) KKT, complementary slackness based method

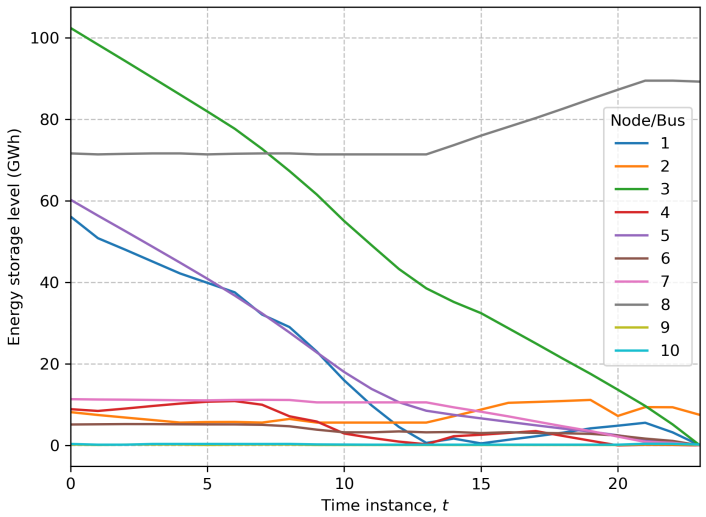

(b) Robust, global consistency method

Fig. 6: Comparison of non-exact recovery method energy level estimates

D. Computational Complexity

Further, timed numerical experiments were performed on time windows of varying length, starting from the test instance `2018-03-01 9:00`, to determine the computational complexity of the dual problem in the observation duration, T. Fig. 7 plots the average solution time, over an appropriate number of iterations, for each duration. It shows that solving the optimisation formulated with `CVXOPT` has a computational complexity in time of approximately $O(T^3)$, thereby validating that the formulation provides a polynomial time method for solving the renewable power system optimisation problem.

However, as discussed in Section IV-E, the dual problem has a 'super sparse' nature in time. Hence, it may be possible to identify a solution algorithm which exploits the sparsity of the problem, and provides an improved computational complexity, thereby making the problem more tractable to solve over long observation windows. One such possibility is the sparse SDP solver algorithm proposed by Madani, Kalbat & Lavaei [47]. The development of computationally efficient algorithms for solving large, sparse optimisation problems is an active research area [48]–[50], whose application to this problem may yield substantial improvements to the solution algorithms.

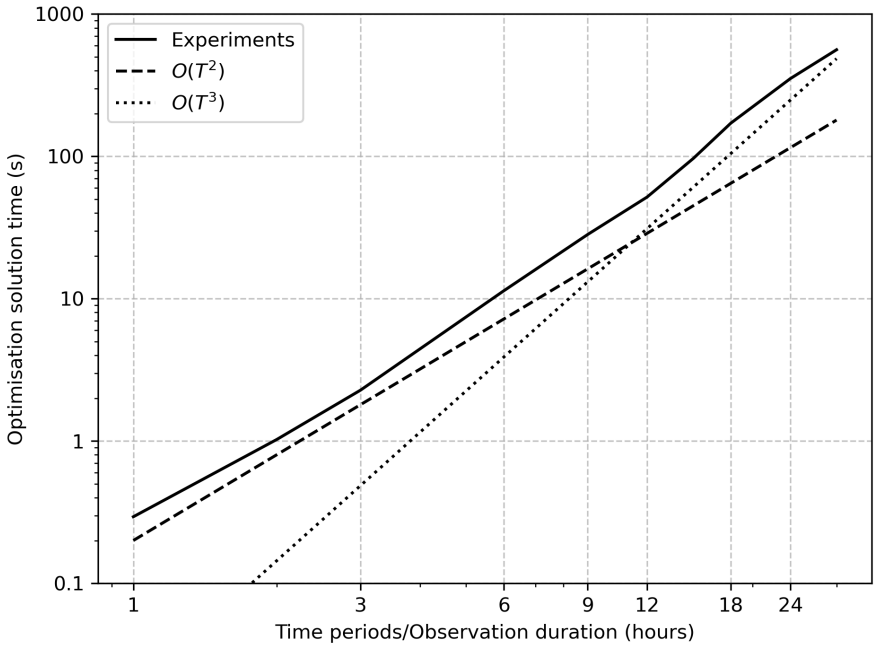

Fig. 7: Solution time of dual problem, (37), on a Quad-Core Intel i3 @ 3.6 GHz

VI. Model Extensions

The optimisation problem formulation in Sections III & IV makes a number of assumptions to simplify the mathematics presented. This Section details how these simplifications can be relaxed, and provides further extensions to the model, demonstrating the technique's ability to tackle more advance renewable power system optimisation problems than the simple storage capacity minimisation task initially studied, whilst retaining convexity and exactness of the dual problem, hence continuing to provide computationally efficient solution methods and solution accuracy guarantees. Justification of the retention of these properties is provided in Section IV-E.

A. Reactive Power

As in the initial model reactive power support is assumed unconstrained and available as required, corresponding to local power factor correction at all buses, this results in reactive power information being lost from the problem during the Lagrangian minimisation, (30d). However, reactive power is a significant contributor to line currents, whose limits are a key localisation effect in network power flow. Hence, the inclusion of reactive power in the model improves the fit to real world network behaviours.

Traditional, induction machine based industrial power factors are typically internally corrected to $\cos(\phi) \approx 0.92 - 0.95$ [51], which results in $Q_{\text{load}} \approx \frac{1}{3} P_{\text{load}}$. Therefore, an approximation of reactive power demand information can be synthesised directly from the real power demand profile if measured data is unavailable. However, this approximation is limited as it fails to capture the variation in load power factors resulting from modern, power electronics based power conditioning systems, which correct power factors close to unity.

Adding constraints on reactive power support of form,

$$Q_{S,n}^{\min} \leq Q_{S,n}[t] \leq Q_{S,n}^{\max} \qquad \forall\, t \in \mathcal{T} \tag{51}$$

introduces additional Lagrange multipliers, dual variables, $\lambda_{n,t}^{QSU}, \lambda_{n,t}^{QSL}$ to the problem, corresponding to the upper and lower bounds respectively, which modify the stationarity KKT conditions (30d) to,

$$\frac{\partial \mathscr{L}}{\partial Q_{S,n}[t]} = \lambda_{n,t}^{QSU} - \lambda_{n,t}^{QSL} - \lambda_{n,t}^{Q} = 0 \qquad \forall\, n \in \mathcal{N},\ t \in \mathcal{T} \tag{52}$$

and introduce additional terms to the dual cost function, given by,

$$\sum_{n,t} \left(\lambda_{n,t}^{QSL} Q_{S,n}^{\min} - \lambda_{n,t}^{QSU} Q_{S,n}^{\max} \right) \tag{53}$$

Hence it can be seen that this modification introduces reactive power information to the optimisation.

Additionally, as discussed later in Section VI-C, the reactive power support capacity, $\hat{Q}_{S,n} = Q_{S,n}^{\max} = -Q_{S,n}^{\min}$, can be introduced as a decision variable, with a corresponding cost term added to the primal cost function, to allow for optimisation of reactive power infrastructure implementation strategies.

B. Round-Trip Efficiency of Storage

Energy storage technologies exhibit a wide range of Round-Trip Efficiencies (RTE) of storage, with Li-ion batteries achieving $85-98\%$ efficiencies, Pumped-Hydro Energy Storage (PHES), $65-85\%$, and Compressed Air Energy Storage (CAES), $50-90\%$, [52]–[54]. Therefore, if significant proportions of total energy usage are arbitraged through storage, the losses incurred may be a significant factor in the overall efficacy of storage. Hence, including RTE in the system dynamics allows for this potentially critical effect to be included in system operation strategy evaluation.

Let $\eta_k^i, \eta_k^o, \eta_k^d(\Delta t)$ be the storage intake efficiency, output efficiency, and self-discharge rate over period Δt, at bus k, respectively. The RTE is given by $\eta_k^{\text{RTE}} = \eta_k^i \eta_k^o$.

The following two relationships are noted,

$$x \leq \min\{a, b\} \implies x \leq a \ \& \ x \leq b \tag{54a}$$

$$x \leq -\max\{a, b\} \implies x \leq \min\{-a, -b\} \tag{54b}$$

Including storage inefficiency in the system dynamics requires the storage power *in-flow* equation, (5), to be adjusted to,

$$P_{E,k}[t] = \begin{cases} \dfrac{1}{\eta_k^i}\left(\dfrac{e_k[t] - \eta_k^d(\Delta t)\cdot e_k[t-1]}{\Delta t}\right) & \text{for intake, } P_{E,k}[t] \geq 0 \\ \eta_k^o\left(\dfrac{e_k[t] - \eta_k^d(\Delta t)\cdot e_k[t-1]}{\Delta t}\right) & \text{for output, } P_{E,k}[t] \leq 0 \end{cases} \tag{55}$$

As,

$$0 < \eta_k^i, \eta_k^o \leq 1 \tag{56}$$

this implies,

$$\frac{1}{\eta_k^i}\left(\frac{e_k[t] - \eta_k^d(\Delta t)\cdot e_k[t-1]}{\Delta t}\right) \geq \eta_k^o\left(\frac{e_k[t] - \eta_k^d(\Delta t)\cdot e_k[t-1]}{\Delta t}\right) \tag{57}$$

Therefore, the power *in-flow* can be re-expressed as,

$$P_{E,k}[t] = \max\left\{\frac{1}{\eta_k^i}\left(\frac{e_k[t] - \eta_k^d(\Delta t)\cdot e_k[t-1]}{\Delta t}\right),\ \eta_k^o\left(\frac{e_k[t] - \eta_k^d(\Delta t)\cdot e_k[t-1]}{\Delta t}\right)\right\} \tag{58}$$

In light of relationships (54a) & (54b), RTE is introduced to the optimisation by the replacement of the slack real power conservation constraints, (21a), with the pair of constraint sets,

$$\text{Tr}\{\boldsymbol{Y}_k W[t]\} \leq P_{G,n}[t] - P_{D,n}[t] - \frac{1}{\eta_k^i}\left(\frac{e_k[t] - \eta_k^d(\Delta t)\cdot e_k[t-1]}{\Delta t}\right) \tag{59a}$$

$$\text{Tr}\{\boldsymbol{Y}_k W[t]\} \leq P_{G,n}[t] - P_{D,n}[t] - \eta_k^o\left(\frac{e_k[t] - \eta_k^d(\Delta t)\cdot e_k[t-1]}{\Delta t}\right) \tag{59b}$$

This adjustment results in two sets of real power Lagrange multipliers/dual variables acting in the dual problem, $\lambda^{P,i}_{n,t}, \lambda^{P,o}_{n,t}$, at most one of which is non-zero in any time instance, as the constraints cannot be binding simultaneously.

C. Full System Operating Costs

As described in Section II, the key aim of the renewable power systems optimisation problem is to identify strategies which yield the minimal overall system operation cost. To achieve this, the formulation is extended to include primal decision variables which fully describe all operational and system development strategies, specifically:

- $\hat{P}^{\text{wind}}_{G,n}$, installed (real power) wind generation capacities[10]
- $\hat{P}^{\text{solar}}_{G,n}$, installed (real power) solar generation capacities
- $\{\ldots\}$, generation capacities of other technologies
- $\hat{Q}_{S,n}$, installed reactive power support capacities
- S_n, installed energy storage capacities

All subject to non-negativity constraints.

In order to introduce the generation capacities as decision variables, the generation power time series for each renewable source must be decomposed into a rated capacity and a mode shape,

$$P_{G,n}[t] = \sum_r P^r_{G,n}[t] \rightarrow \sum_r \Big(\underbrace{\tilde{P}^r_{G,n}[t]}_{\text{mode shape}} \times \underbrace{\hat{P}^r_{G,n}}_{\text{rated capacity}} \Big) \tag{60}$$

The objective function is then modified to represent the total cost of system operation per annum,

$$\sum_{n\in\mathcal{N}} \Big(c_S S_n + c^{\text{wind}}_P \hat{P}^{\text{wind}}_{G,n} + c^{\text{solar}}_P \hat{P}^{\text{solar}}_{G,n} + \ldots + c_{QS}\hat{Q}_{S,n} \Big) \tag{61}$$

where the constants c_x are the appropriate per unit, per annum, costs of system infrastructure.

Through this extension, the recovered optimal values of the primal variables provide complete information about the minimal cost system development and operation strategies for the renewable power system. Further, the optimal cost, $d^* = p^*$, can be used to forecast the future cost of fully renewable power provision, from which effective economic and policy strategies can be inferred, for instance carbon pricing.

[10] Note, reactive power generation capacity is derived from real power capacity, based off the operational physics of each technology.

D. Network Topology Optimisation

The literature shows that increased grid interconnection can both improve security of supply in high penetration renewable energy systems [55], and reduce system operation costs [56], [57]. It is therefore desirable to extend the proposed optimisation to include network bus connections as decision variables. However, this poses two significant challenges. Firstly, said decision variables are binary, resulting in a mixed integer program, and making the problem both non-convex and combinatorially hard [58]. Secondly, relaxation from integer decision variables still results in a non-convex optimisation, as those relaxed decision variables act in the network admittance matrix, Y, which then determines the network characteristic matrices $\boldsymbol{Y}_n, \bar{\boldsymbol{Y}}_n, \boldsymbol{Y}_{lm}, \bar{\boldsymbol{Y}}_{lm}$. Hence, the trace terms $\mathrm{Tr}\{\boldsymbol{Y}_n W[t]\}, \ldots$ involve products of two decision variables. This means that the primal constraints (21a)–(21c) are no longer linear, as they contain quadratic terms, and hence Optimisation D is no longer a SDP, and no longer convex.

However, considering the topology of electrical transmission networks and their sparsity, see Fig. 1, and the practical considerations of line transmission line construction, it is likely that the domain of feasible network configurations will be limited. Therefore, an exhaustive search, evaluating the extended optimisation from Section VI-C for each configuration, will likely be tractable, and allow for the optimal network connectivity development strategy to determined.

The binary connection variables can be extended to non-negative integer variables representing the number of lines directly connecting each pair of buses. This enables optimisation over the restricted domain of feasible apparent power line capacities, $S_{lm}^{\max}$, to be performed in a similar manner.

E. Combined Traditional & Renewable Generation Power Systems

Extension to a mixed generation strategy power system including dispatchable Non-Renewable (NR) generation assets, requires adjustment of the bus power generation term to,

$$P_{G,n}[t] = \sum_r \left(\tilde{P}_{G,n}^r[t] \hat{P}_{G,n}^r \right) + P_{G,n}^{\mathrm{NR}}[t] \tag{62}$$

subject to constraints,

$$0 \leq P_{G,n}^{\mathrm{NR}}[t] \leq \hat{P}_{G,n}^{\mathrm{NR}} \tag{63}$$

where the additional primal variables, $P_{G,n}^{\mathrm{NR}}[t]$ & $\hat{P}_{G,n}^{\mathrm{NR}}$, are the instantaneous NR generation power at time t, and NR generation capacity, at node n, respectively.

The following terms are added to the primal cost function,

$$\sum_n c_{\mathrm{NR}} \hat{P}_{G,n}^{\mathrm{NR}} + \sum_{n,t} c_{\mathrm{CO_2}} P_{G,n}^{\mathrm{NR}}[t] \left(\frac{y(\Delta t)}{T} \right) \tag{64}$$

where c_{NR} is the per unit, per annum cost of NR capacity, $c_{\mathrm{CO_2}}$, the carbon price per MWh of NR electricity generated, and $y(\Delta t)$, the number of time periods Δt per year. This form of cost accounts for both the fixed costs of NR backup generation capacity, and the external, environmental, costs of its usage, via the carbon pricing term.

VII. Conclusion

This work has studied the renewable power system optimisation problem, and investigated how full complexity power network physics can be introduced to the optimisation whilst retaining convexity, in order to exploit the computational efficiency, global optimality, and solution accuracy guarantees it provides. It sought to bridge the gap between existing convex formulations for solving classical, non-linear MOPF problems, and state-of-the-art, linear power system optimisation tools, by developing a convex MOPF formulation for renewable power system infrastructure optimisation. Such a formulation was achieved by extending those proposed in [4] & [5], expressing the optimisation as a SDP via the dual of a rank relaxation. Further, necessary and sufficient conditions for zero duality gap, and hence exactness of the relaxation dual, were proved, thus providing a convex technique for solving the original MOPF problem. This proof followed from the separability in time of the aggregate Lagrange multiplier matrices associated with the primal voltage matrix variables. Additionally, these aggregate Lagrange multipliers, dual variables, were found to be unaltered by the addition of further affine system dynamics, thus leaving the nature of dual problem unchanged, and retaining the conditions for exactness. The time separability of the dual variables also led to the dual problem having a 'super sparse' structure, which may be able to be exploited by a dedicated solver to provide a highly computationally efficient solution method. Via numerical experiments, it was shown that the exactness conditions were able to be satisfied by the topology of a simplified model of the UK power transmission network, Fig. 1, and the implications of this on the ability to obtain arbitrarily accurate approximate solutions via the ε-modified problem discussed. These experiments also verified the formulation to provide a polynomial time method for determining the global optimum solution of the MOPF problem, with the computational complexity in time found to be $O(T^3)$. Finally, it was demonstrated that the simplified formulation presented can be extended to a fully-featured power system optimisation tool, whilst retaining its convexity.

Renewable power system optimisation has the ability to provide both substantial reductions in the overall cost of system operation, and improvements in security of supply, when using fully renewable electricity generation, via the identification of effective system implementation and operation strategies. However, modern power system optimisation tools do not account for full complexity power network physics, of which the non-linear line losses may constitute a critical localisation effect in large-scale power transmission systems. This work has demonstrated that convexification techniques from classical OPF literature provide a pathway for the development of computationally efficient, convex formulations of the full complexity renewable power system optimisation problem. Further research is required to determine the circumstances under which the conditions for exactness are satisfied, and whether the sparsity property of the dual optimisation can be exploited to reduce the computational complexity of the solution method.

REFERENCES

[1] T. Brown, J. Hörsch, and D. Schlachtberger, "PyPSA: Python for Power System Analysis," *Journal of Open Research Software*, vol. 6, no. 4, 2018. [Online]. Available: https://doi.org/10.5334/jors.188

[2] J. D. Jenkins and N. A. Sepulveda, "Enhanced decision support for a changing electricity landscape: the GenX configurable electricity resource capacity expansion model," *An MIT Energy Initiative Working Paper. https://energy.mit.edu/wpcontent/uploads/2017/10/Enhanced-Decision-Support-for-a-Changing-Electricity-Landscape.pdf*, 2017.

[3] H. G. Svendsen and O. C. Spro, "PowerGAMA: A new simplified modelling approach for analyses of large interconnected power systems, applied to a 2030 Western Mediterranean case study," *Journal of Renewable and Sustainable Energy*, vol. 8, no. 5, p. 055501, 2016.

[4] J. Lavaei and S. H. Low, "Zero duality gap in optimal power flow problem," *IEEE Transactions on Power Systems*, vol. 27, no. 1, pp. 92–107, 2011.

[5] D. Gayme and U. Topcu, "Optimal power flow with large-scale storage integration," *IEEE Transactions on Power Systems*, vol. 28, no. 2, pp. 709–717, 2012.

[6] J. Lavaei and S. H. Low, "Convexification of optimal power flow problem," in *2010 48th Annual Allerton Conference on Communication, Control, and Computing (Allerton)*, 2010, pp. 223–232.

[7] J. Lavaei, "Zero duality gap for classical opf problem convexifies fundamental nonlinear power problems," in *Proceedings of the 2011 American Control Conference*, 2011, pp. 4566–4573.

[8] T. Liu, B. Sun, and D. H. Tsang, "Rank-one solutions for sdp relaxation of qcqps in power systems," *IEEE Transactions on Smart Grid*, vol. 10, no. 1, pp. 5–15, 2017.

[9] B. Ghaddar, J. Marecek, and M. Mevissen, "Optimal power flow as a polynomial optimization problem," *IEEE Transactions on Power Systems*, vol. 31, no. 1, pp. 539–546, 2015.

[10] D. Kourounis, A. Fuchs, and O. Schenk, "Toward the next generation of multiperiod optimal power flow solvers," *IEEE Transactions on Power Systems*, vol. 33, no. 4, pp. 4005–4014, 2018.

[11] NCAS British Atmospheric Data Centre, "Met Office (2012): Met Office Integrated Data Archive System (MIDAS) Land and Marine Surface Stations Data (1853-current)," http://catalogue.ceda.ac.uk/uuid/220a65615218d5c9cc9e4785a3234bd0, Jan. 2021.

[12] Y.-M. Saint-Drenan, R. Besseau, M. Jansen, I. Staffell, A. Troccoli, L. Dubus, J. Schmidt, K. Gruber, S. G. Simões, and S. Heier, "A parametric model for wind turbine power curves incorporating environmental conditions," *Renewable Energy*, vol. 157, pp. 754 – 768, 2020. [Online]. Available: http://www.sciencedirect.com/science/article/pii/S0960148120306613

[13] aqreed, "solarpy: Solar radiation model based on Duffie & Beckman "Solar energy thermal processes" (1974)," https://pypi.org/project/solarpy/, Sep. 2019.

[14] J. Carpentier, "Contribution to the economic dispatch problem," *Bulletin de la Societe Francoise des Electriciens*, vol. 3, no. 8, pp. 431–447, 1962.

[15] K. Pandya and S. Joshi, "A survey of optimal power flow methods," *Journal of Theoretical and Applied Information Technology*, vol. 4, p. 450–458, 01 2008.

[16] J. Momoh, R. Adapa, and M. El-Hawary, "A review of selected optimal power flow literature to 1993. i. nonlinear and quadratic programming approaches," *IEEE Transactions on Power Systems*, vol. 14, no. 1, pp. 96–104, 1999.

[17] J. Momoh, M. El-Hawary, and R. Adapa, "A review of selected optimal power flow literature to 1993. ii. newton, linear programming and interior point methods," *IEEE Transactions on Power Systems*, vol. 14, no. 1, pp. 105–111, 1999.

[18] M. B. Maskar, A. Thorat, and I. Korachgaon, "A review on optimal power flow problem and solution methodologies," in *2017 International Conference on Data Management, Analytics and Innovation (ICDMAI)*. IEEE, 2017, pp. 64–70.

[19] J. A. Momoh, *Electric power system applications of optimization*. CRC press, 2000.

[20] R. Jabr, "Radial distribution load flow using conic programming," *IEEE Transactions on Power Systems*, vol. 21, no. 3, pp. 1458–1459, 2006.

[21] R. A. Jabr, "Optimal power flow using an extended conic quadratic formulation," *IEEE Transactions on Power Systems*, vol. 23, no. 3, pp. 1000–1008, 2008.

[22] X. Bai, H. Wei, K. Fujisawa, and Y. Wang, "Semidefinite programming for optimal power flow problems," *International Journal of Electrical Power & Energy Systems*, vol. 30, no. 6-7, pp. 383–392, 2008.

[23] S. H. Low, "Convex relaxation of optimal power flow—part i: Formulations and equivalence," *IEEE Transactions on Control of Network Systems*, vol. 1, no. 1, pp. 15–27, 2014.

[24] ——, "Convex relaxation of optimal power flow—part ii: Exactness," *IEEE Transactions on Control of Network Systems*, vol. 1, no. 2, pp. 177–189, 2014.

[25] H. Yang and H. Nagarajan, "Optimal power flow in distribution networks under stochastic $N-1$ disruptions," *Electric Power Systems Research*, vol. 189, p. 106689, 2020. [Online]. Available: https://www.sciencedirect.com/science/article/pii/S0378779620304922

[26] A. Gopalakrishnan, A. U. Raghunathan, D. Nikovski, and L. T. Biegler, "Global optimization of multi-period optimal power flow," in *2013 American Control Conference*, 2013, pp. 1157–1164.

[27] S. Boyd, S. P. Boyd, and L. Vandenberghe, *Convex optimization*. Cambridge university press, 2004.

[28] K. M. Anstreicher, "On convex relaxations for quadratically constrained quadratic programming," *Mathematical programming*, vol. 136, no. 2, pp. 233–251, 2012.

[29] F. Zhang, *The Schur complement and its applications*. Springer Science & Business Media, 2006, vol. 4.

[30] D. Kleinman and M. Athans, "The design of suboptimal linear time-varying systems," *IEEE Transactions on Automatic Control*, vol. 13, no. 2, pp. 150–159, 1968.

[31] Z. Hu, F. Nie, R. Wang, and X. Li, "Low rank regularization: A review," *Neural Networks*, 2020.

[32] P. Gahinet and A. Nemirovski, "The projective method for solving linear matrix inequalities," *Mathematical programming*, vol. 77, no. 1, pp. 163–190, 1997.

[33] E. De Klerk, *Aspects of semidefinite programming: interior point algorithms and selected applications*. Springer Science & Business Media, 2006, vol. 65.

[34] W. Medjroubi, C. Matke, and D. Kleinhans. (2016, Jul.) Scigrid–an open source reference model for the european transmission network (v0.2). [Online]. Available: http://www.scigrid.de

[35] B. Wiegmans. (2016, Jun.) Gridkit extract of entso-e interactive map. [Online]. Available: https://doi.org/10.5281/zenodo.55853

[36] W. Heitkoetter, W. Medjroubi, T. Vogt, and C. Agert, "Comparison of open source power grid models—combining a mathematical, visual and electrical analysis in an open source tool," *Energies*, vol. 12, no. 24, 2019. [Online]. Available: https://www.mdpi.com/1996-1073/12/24/4728

[37] M. Andersen, J. Dahl, and L. Vandenberghe. (2012) CVXOPT: A Python package for convex optimization, version 1.2.5. [Online]. Available: http://cvxopt.org

[38] M. Andersen, J. Dahl, Z. Liu, L. Vandenberghe, S. Sra, S. Nowozin, and S. Wright, "Interior-point methods for large-scale cone programming," *Optimization for machine learning*, vol. 5583, 2011.

[39] B. O'Donoghue, E. Chu, N. Parikh, and S. Boyd, "Conic optimization via operator splitting and homogeneous self-dual embedding," *Journal of Optimization Theory and Applications*, vol. 169, no. 3, pp. 1042–1068, June 2016. [Online]. Available: http://stanford.edu/~boyd/papers/scs.html

[40] ——, "SCS: Splitting conic solver, version 2.1.3," https://github.com/cvxgrp/scs, Nov. 2019.

[41] S. Diamond and S. Boyd, "CVXPY: A Python-embedded modeling language for convex optimization," *Journal of Machine Learning Research*, vol. 17, no. 83, pp. 1–5, 2016.

[42] A. Agrawal, R. Verschueren, S. Diamond, and S. Boyd, "A rewriting system for convex optimization problems," *Journal of Control and Decision*, vol. 5, no. 1, pp. 42–60, 2018.

[43] ENTSO-E, "Transmission system map," https://www.entsoe.eu/data/map/, Jan. 2019.

[44] Siemens, "400kV Overhead Transmission Line Protection," Tech. Rep., 2005. [Online]. Available: https://www.quad-industry.com/titan_img/ecatalog/Appl_13_400kV_OHL_Protection_en.pdf

[45] National Grid, "Annex: NGET_A11.11 Transmission Loss Strategy," Tech. Rep., Dec. 2019. [Online]. Available: https://www.nationalgrid.com/uk/electricity-transmission/document/132276/download

[46] GridWatch, "GridWatch Database (2011-current)," https://www.gridwatch.templar.co.uk/download.php, Sep. 2020.

[47] R. Madani, A. Kalbat, and J. Lavaei, "A low-complexity parallelizable numerical algorithm for sparse semidefinite programming," *IEEE Transactions on Control of Network Systems*, vol. 5, no. 4, pp. 1898–1909, 2018.

[48] J. R. Bunch and D. J. Rose, *Sparse matrix computations*. Academic Press, 2014.

[49] N. Wu, G. Kenway, C. A. Mader, J. Jasa, and J. R. Martins, "pyoptsparse: A python framework for large-scale constrained nonlinear optimization of sparse systems," *Journal of Open Source Software*, vol. 5, no. 54, p. 2564, 2020.

[50] Y. H. S. K. Xie, "Optimal spinning reserve allocation with full ac network constraints via a nonlinear interior point method," *Electric Machines & Power Systems*, vol. 28, no. 11, pp. 1071–1090, 2000. [Online]. Available: https://doi.org/10.1080/073135600449116

[51] J. Ware, "Power factor correction (pfc)," *IET Wiring Matters*, no. 18, pp. 22–24, 2006, [Online]. Available: https://electrical.theiet.org/media/1687/power-factor-correction-pfc.pdf.

[52] International Renewable Energy Agency (IRENA), "Electricity storage and renewables: Costs and markets to 2030," Oct. 2017. [Online]. Available: https://www.irena.org/-/media/Files/IRENA/Agency/Publication/2017/Oct/IRENA_Electricity_Storage_Costs_2017.pdf

[53] D. Akinyele and R. Rayudu, "Review of energy storage technologies for sustainable power networks," *Sustainable Energy Technologies and Assessments*, vol. 8, pp. 74–91, 2014.

[54] A. K. Rohit, K. P. Devi, and S. Rangnekar, "An overview of energy storage and its importance in indian renewable energy sector: Part i–technologies and comparison," *Journal of Energy Storage*, vol. 13, pp. 10–23, 2017.

[55] T. Jamasb and M. Pollitt, "Security of supply and regulation of energy networks," *Energy Policy*, vol. 36, no. 12, pp. 4584–4589, 2008.

[56] M. Child, C. Kemfert, D. Bogdanov, and C. Breyer, "Flexible electricity generation, grid exchange and storage for the transition to a 100% renewable energy system in europe," *Renewable energy*, vol. 139, pp. 80–101, 2019.

[57] M. Á. Lynch, R. S. Tol, and M. J. O'Malley, "Optimal interconnection and renewable targets for north-west europe," *Energy Policy*, vol. 51, pp. 605–617, 2012.

[58] A. Schrijver, *Theory of linear and integer programming*. John Wiley & Sons, 1998.

Appendices

APPENDIX I
TECHNICAL APPENDICES

A. Recovery of Voltage States for Exact Time Instances

The method for recovering the bus voltage states at a time instance, t, which satisfies the null space condition for exactness, is based on Property 1 from Corollary 1 of [4],

"If the zero-duality-gap condition [is satisfied;] given any nonzero vector $[X_1^T\ X_2^T]^T$ in the null space of $A(x^{\text{opt}}, r^{\text{opt}})$, there exist two real-valued scalars ζ_1 and ζ_2 such that $\boldsymbol{V}^{\text{opt}} = (\zeta_1 + \zeta_2 i)(X_1 + X_2 i)$ is a global optimum of the OPF problem."

Extending to the multi-period case, this result applies independently to each time instance t which satisfies its exactness condition.

Therefore,

$$\begin{aligned}\boldsymbol{V}[t]^{\text{opt}} &= (\zeta_1[t] + \zeta_2[t]\mathbf{j})(v_1[t] + v_2[t]\mathbf{j}) \\ &= (\zeta_1[t]v_1[t] - \zeta_2[t]v_2[t]) + (\zeta_1[t]v_2[t] + \zeta_2[t]v_1[t])\mathbf{j}\end{aligned} \tag{65}$$

for any non-zero vector $[v_1[t]^T\ v_2[t]^T]^T$ in the null space of $A(\boldsymbol{\lambda}^{\text{opt}}, \boldsymbol{R}^{\text{opt}}, t)$.

As the complex voltage of the reference bus, node 1, is known,

$$V_1[t] = V_{\text{nom}}\angle 0^\circ \qquad \forall\, t \in \mathcal{T} \tag{66}$$

Therefore,

$$\text{Im}\left\{\boldsymbol{V}[t]^{\text{opt}}_{\{1\}}\right\} = 0 \tag{67}$$

$$\implies \text{Im}\left\{\left((\zeta_1[t] + \zeta_2[t]\mathbf{i})(v_1[t] + v_2[t]\mathbf{i})\right)_{\{1\}}\right\} = 0 \tag{68}$$

$$\implies \zeta_1[t]v_2[t]_{\{1\}} + \zeta_2[t]v_1[t]_{\{1\}} = 0 \tag{69}$$

$$\therefore \qquad \zeta_2[t]^2 = \left(\frac{v_2[t]_{\{1\}}}{v_1[t]_{\{1\}}}\right)^2 \zeta_1[t]^2 \tag{70}$$

introducing the notation, $\boldsymbol{u}_{\{i\}} = u_i$, the i^{th} element of the vector $\boldsymbol{u}$.

Noting that $\text{Tr}\{M_n W[t]\} = \left|V_n[t]\right|^2$, the complementary slackness KKT conditions corresponding to primal constraints (21d) become,

$$\lambda^{VL}_{n,t}\left((V_n^{\min})^2 - \left|V_n[t]^{\text{opt}}\right|^2\right) = 0 \tag{71a}$$

$$\lambda^{VU}_{n,t}\left(\left|V_n[t]^{\text{opt}}\right|^2 - (V_n^{\max})^2\right) = 0 \tag{71b}$$

A node $k \in \mathcal{N}$ such that $\max\{\lambda^{VL}_{k,t}, \lambda^{VU}_{k,t}\} > 0$ is identified, i.e. a node at which one of the voltage magnitude constraints is active. The voltage magnitude at this bus is therefore known via complementary slackness. Let this voltage magnitude squared be $(V_k^b)^2 \in \{(V_k^{\min})^2, (V_k^{\max})^2\}$.

Hence,

$$\left|V_k[t]^{\text{opt}}\right|^2 = \left|\zeta_1[t] + \zeta_2[t]\mathbf{j}\right|^2 \left|v_1[t]_{\{k\}} + v_2[t]_{\{k\}}\mathbf{j}\right|^2 = (V_k^b)^2 \tag{72}$$

$$\implies \zeta_1[t]^2 + \zeta_2[t]^2 = \frac{(V_k^b)^2}{v_1[t]_{\{k\}}^2 + v_2[t]_{\{k\}}^2} \tag{73}$$

Solving the two linear equations (70) & (73) yields the two scalars $\zeta_1[t], \zeta_2[t]$,

$$\zeta_1[t] = \sqrt{\left(1 + \left(\frac{v_2[t]_{\{1\}}}{v_1[t]_{\{1\}}}\right)^2\right)^{-1} \left(\frac{(V_k^b)^2}{v_1[t]_{\{k\}}^2 + v_2[t]_{\{k\}}^2}\right)} \tag{74a}$$

$$\zeta_2(t) = -\frac{v_2[t]_{\{1\}}}{v_1[t]_{\{1\}}}\zeta_1[t] \tag{74b}$$

Finally, the sign of the vector is altered if required, to ensure that the reference bus has a positive real voltage, i.e. a phase angle of 0 rather than 180,

$$V[t]^{\text{opt}} = (\zeta_1[t] + \zeta_2[t]\mathbf{j})(v_1[t] + v_2[t]\mathbf{j}) \cdot \text{sign}(\zeta_1[t]v_1[t]_{\{1\}} - \zeta_2[t]v_2[t]_{\{1\}}) \tag{75}$$

Note that if there does not exist $k \in \mathcal{N}$ such that $\max\{\lambda_{k,t}^{VL}, \lambda_{k,t}^{VU}\} > 0$, then the node voltage reconstruction method fails in this time instance.

B. Storage Energy Level Reconstruction

The optimal voltage matrix variables $W[t]^{\text{opt}}$ fully define the power flows through the network during optimal operation of the system over the time window $\mathcal{T}$. From these, the storage power flows, $P_{E,n}[t]^{\text{opt}}$, are determined, and thus the energy levels, $e_n[t]$, and storage capacities, S_n, recovered. Further, as the power flow to/from each bus is calculable, all nodes can be evaluated independently, as the full network effect is encapsulated by $W[t]^{\text{opt}}$.

The reconstruction strategy involves two stages:

i) An initial pass over some subset of the time window, $t \in \{1, \ldots, \tau \leq T\}$, which tracks the change in energy level, until a time instance is reached at which the absolute value of the energy level is known. From the cumulative energy difference, $\Delta e_n[\tau]$, and known absolute level, $e_n[\tau]$, the energy capacity S_n is computed.

ii) A secondary pass, which computes the energy levels at each time instance recursively forwards in time, starting at $e_n[0] = \alpha S_n$.

For time instances where $\lambda^P_{n,t} \neq 0$, the real power conservation constraints are known to be binding. From the complementary slackness KKT conditions corresponding to primal constraints (21a),

$$\lambda^P_{n,t}\left(\mathrm{Tr}\{\mathbf{Y}_n W[t]\} - P_{G,n}[t] + P_{D,n}[t] + (e_n[t] - e_n[t-1])/\Delta t\right) = 0 \tag{76}$$

the following update rule for the storage energy level is derived,

$$e_n[t] = e_n[t-1] - \Delta t\left(\mathrm{Tr}\{\mathbf{Y}_n W[t]\} + (P_{D,n}[t] - P_{G,n}[t])\right) \quad \text{for } t : \lambda^P_{n,t} \neq 0 \tag{77}$$

The complementary slackness KKT condition, $-\lambda^S_n S_n = 0$, corresponding to the non-negativity of storage capacity primal constraints, (21f), are used to identify nodes $n : \lambda^S_n \neq 0$, for which $S_n = 0$, in order to save computation.

Complementary Slackness Method:

The main reconstruction method utilises the Lagrange multipliers $\lambda^{eL}_{n,\tau}, \lambda^{eU}_{n,\tau}$ to identify known absolute energy levels via the complementary slackness KKT conditions corresponding to the energy level validity primal constraints, (21e),

$$-\lambda^{eL}_{n,t} e_n[t] = 0 \tag{78a}$$

$$\lambda^{eU}_{n,t}(e_n[t] - S_n) = 0 \tag{78b}$$

The total energy level change from the initial state of charge, $\Delta e_n[t]$, is computed recursively forwards in time using the update rule (77), until a time instance τ is reached such that $\min\{\lambda^{eL}_{n,\tau}, \lambda^{eU}_{n,\tau}\} = 0$, i.e. one of the constraints is binding.

At this $t = \tau$, the absolute energy level is known,

$$e_n[\tau] = \begin{cases} 0 & \text{if } \lambda^{eL}_{n,\tau} \neq 0 \\ S_n & \text{if } \lambda^{eU}_{n,\tau} \neq 0 \end{cases} \tag{79}$$

From this absolute energy level, and the computed relative energy level, the storage capacity is determined,

$$S_n = \begin{cases} \left|\Delta e_n[\tau]\right| / \alpha_n & \text{if } \lambda^{eL}_{n,\tau} \neq 0 \\ \left|\Delta e_n[\tau]\right| / (1 - \alpha_n) & \text{if } \lambda^{eU}_{n,\tau} \neq 0 \end{cases} \tag{80}$$

This is valid only for $\alpha_n \neq 1$. For the case $\alpha_n = 1$, a time instance for which $\lambda^{eL}_{n,\tau} \neq 0$ is sought to compute S_n. Additionally, the case $\lambda^{eL}_{n,\tau} \neq 0$ & $\lambda^{eU}_{n,\tau} \neq 0$ is valid iff $S_n = 0$.

This reconstruction method is described by the following algorithm,

Algorithm 1: Complementary slackness based energy level reconstruction

initialisation;
$t \leftarrow 0$;
$\Delta e \leftarrow 0$;

first pass;
while $\lambda_{n,t}^{eL} = 0$ & $\lambda_{n,t}^{eU} = 0$ **do**
  $\Delta e \leftarrow \Delta e - \Delta t \left(\mathrm{Tr}\{\mathbf{Y}_n W[t]\} + (P_{D,n}[t] - P_{G,n}[t])\right)$;
  $t \leftarrow t + 1$;
end

compute storage capacity;
if $\lambda_{n,t}^{eL} \neq 0$ **then**
  $S_n \leftarrow \left|\Delta e_n[\tau]\right| / \alpha_n$
else if $\lambda_{n,t}^{eU} \neq 0$ **then**
  $S_n \leftarrow \left|\Delta e_n[\tau]\right| / (1 - \alpha_n)$
end

second pass;
$e_n[0] \leftarrow \alpha_n S_n$;
for $t \leftarrow 1$ **to** T **do**
  if $\lambda_{n,t}^{P} = 0$ **then**
    $e_n[t] \leftarrow e_n[t-1] - \Delta t \left(\mathrm{Tr}\{\mathbf{Y}_n W[t]\} + (P_{D,n}[t] - P_{G,n}[t])\right)$
  else
    raise error;
  end
end

Note that time instances for which $\lambda_{n,t}^{P} = 0$ do not obey the update rule (77). However, such an occurrence corresponds to the price of real power at that node at that time instance, represented by $\lambda_{n,t}^{P}$, being zero. Therefore, by physical considerations, this should always coincide with $\lambda_{n,t}^{eU} \neq 0$, as otherwise, the excess real power would be bought by the storage unit at some non-zero price. Therefore, the update rule can be applied as an approximation, incurring some potentially small error, and the storage capacity determine from that approximate energy level.

Global Consistency Method:

Due to the nature of numerical solvers, the identification of 'zero' Lagrange multiplier values can involve large uncertainty. Therefore, an alternative reconstruction method which is robust to such uncertainty is developed, to provide improved estimates of S_n in said scenarios.

In this method, the full sequence of energy level differences,

$$\{\delta e_n[t]\}_{t=1}^{T} = \{e_n[t] - \alpha_n S_n\}_{t=1}^{T}$$

is computed recursively forwards in time in terms of S_n, using the update rule (77).

From this time series, the storage capacity is determined as,

$$S_n = \max\left\{ \frac{\left|\min_t(\delta e_n[t])\right|}{\alpha_n} \,,\; \frac{\max_t(\delta e_n[t])}{1-\alpha_n} \,,\; \left|\max_t(\delta e_n[t])\right| + \left|\min_t(\delta e_n[t])\right| \right\} \tag{81}$$

for $\alpha_n \neq 1$. For the case $\alpha_n = 1$, the undefined middle option is excluded. This expression is derived from consideration of the three possible modes of energy level trajectory of the storage units, shown in Fig. 8:

1) $e_n[t'] = 0$ binding for some t' only
2) $e_n[t'] = S_n$ binding for some t' only
3) Both constraints binding over the time window

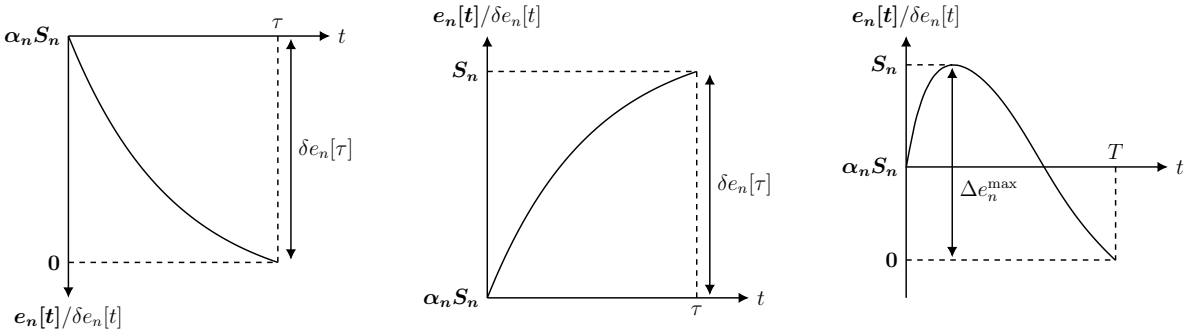

Fig. 8: Storage unit energy level trajectory modes

C. Online Appendix

The online appendix, hosted at `http://mal84.user.srcf.net/iib-project/online-appendices.html`, provides details of the data sources, data preparation methodology, and code listings for the dual optimisation and solution recovery implementations used in the numerical experiments, as well as some 'back of the envelope' calculations which motivate the development of optimisation formulations which account for full complexity, non-linear line losses. However, it is not submitted formally for consideration as part of the Master's project report, and is provided purely as reference material and a host for interactive figures and code listings.

Appendix II
Code Listings

Code listings for a Python-based implementation of the formulated optimisation and solution strategies in Section IV, and the definition of the test network used in the numerical experiments in Section V, are provided in the following files respectively, hosted in the online appendix:

A. `op_code.py`

B. `test_net.py`

APPENDIX III
COVID-19 DISRUPTION

There were no overt disruptions to the work resulting from the COVID-19 pandemic.

APPENDIX IV
RISK ASSESSMENT RETROSPECTIVE

The risk assessment was found to be appropriate, as the necessary ergonomic precautions were taken, and computer-work related strain injuries were avoided.